High Resolution Seismic Reflection Survey near SPR Surface Collapse Feature at Weeks Island, Louisiana

by

Richard D. Miller
Jianghai Xia
Joe M. Anderson
David R. Laflen
Jeffrey M. Erickson
Patricia M. Acker
Mary C. Brohammer

of the
Kansas Geological Survey

and

Don W. Steeples
Ross A. Black

of the
Department of Geology
University of Kansas

expanded final report submitted to
Sandia National Laboratory
Albuquerque, NM
on work completed for the
United States Department of Energy under
Contract DE-AC04-94AL85000

Open-file Report No. 94-25

August 10, 1994

Summary

Shallow, high resolution seismic reflection techniques detected the subsurface expression of a 40 ft wide and 30 ft deep sinkhole above DOE's Strategic Petroleum Reserve (SPR) storage cavities at Weeks Island, Louisiana. The underground cavities that presently hold 73 million barrels of crude oil are two levels of a former room and pillar salt mine. The mine is within a salt dome that at the sinkhole is approximately 180 ft below the ground surface and responsible for the more than 125 ft of topographic uplift that produced Weeks Island. Four nominal 180 shot-point, 24-fold P-wave CDP lines acquired with 8 ft station spacing possess interpretable reflections with an average dominant frequency of approximately 80 Hz and apparent NMO velocities ranging from 1350 to 2100 ft/sec. The field recording parameters and quality control were based on the reflection interpreted during walkaway tests to be from a reflector about 150 ft deep. This coherent reflection event interpretable on all four lines is dramatically altered on the east/west line in the proximity of the sinkhole. An offset in the prominent reflection interpretable on all four lines traces a southwest/northeast trend across the study area. The disturbed reflection on the east/west line, presumed associated with the sinkhole, structurally resembles a chimney type feature or possibly a water table drawdown.

Introduction

This seismic reflection survey was designed to detect and delineate geologic or hydrologic features associated with the small sinkhole discovered on May 18, 1992, as well as identify areas potentially susceptible to subsidence above the SPR storage cavities. The two-level underground cavities, presently holding 73 million barrels of crude oil, are a former room and pillar salt mine. The old mineworks range in depth from about 500 ft to more than 700 ft below the ground surface. The top of the salt dome is approximately 180 ft below the ground surface at the sinkhole and is responsible for the more than 125 ft of topographic uplift that produced Weeks Island. The water table near the sinkhole is about 90 ft below the ground surface. The absence of a cap rock (at least in a classic sense) leaves the salt boundaries of this dome in direct contact with overlying unconsolidated marine sediments. At the time of this survey the sinkhole was approximately 35-40 ft in diameter, slightly more than 30 ft deep, and had surface expression within 50 ft of the south side of Morton Road (Figure 1).

The proposed high-resolution seismic survey originally consisted of five lines, each approximately 1500 ft in length: four P-wave (compressional wave) lines and one S-wave (shear wave) line. The lines were laid out to maximize the potential of imaging the subsurface expression of the present sinkhole and to identify other areas that might be susceptible to subsidence. The primary target was the top of the salt dome. The secondary target was the water table, followed by structural or stratigraphic signatures within the salt dome. Dissolution features associated with evaporite beds have produced easily interpreted signatures on shallow seismic sections (Miller et al., 1993; Steeples and Miller, 1987; Steeples et al., 1986). Based on work at other salt domes (Black and Voigt, 1982; *Leading Edge*, August 1994 issue), a very irregular salt/sediment contact is likely at this site. Direct imaging of the salt-sediment contact has proved challenging on previous surveys at this salt dome (Kinsland and Rutter, 1994). Irregularities in the surface of the salt associated with either dissolution or joints and their expression in overlying sediments are of particular interest.

The acquisition portion of the seismic reflection survey was conducted between March 2 and 4, 1994. The project consisted of several walkaway noise tests and four nominal 180 shotpoint, 24-fold P-wave CDP lines (Figure 1). The surface conditions varied from heavily wooded (hand-cleared 5 ft wide path) to manicured lawn to asphalt roads. Some secondary clearing was necessary along wooded paths previously cleared for elevation surveying. The asphalt and gravel roads were obstacles that not only resulted in minor reductions in fold but also provided a source for traffic noise. No shots were recorded while vehicles were close enough to active recording stations to produce more than 0.1 mV peak-to-peak of background noise. Underground utilities including a petroleum pipeline, a propane pipeline, high voltage power lines, a fiber optic communications link, standard telephone lines, and water lines inhibited continuous coverage across several sections of the four lines. The ground surface was damp, with several significant topographic and cultural obstacles including ditches, relatively steep terraces, partially buried foundations from previous surface structures, and about 55 ft of relative elevation change on lines 1, 2, and 3. The field recording parameters and quality control were based on the 150 ft deep reflector interpreted during walkaway tests on the north end of line 1. Future borehole logging, both geologic and geophysical, based on the surface seismic data should greatly enhance the quality and quantity of seismic interpretations.

Data Acquisition

Data for this study were acquired on a 48-channel EG&G Geometrics 2401x seismograph. The seismograph amplifies, filters (analog), digitizes the analog signal into a 15-bit word, and stores the digital information in a demultiplexed format. Analog filters have an 18 dB/octave rolloff from the selected -3 dB point. The 1/2 msec sampling interval resulted in a record length of 500 msec and a 1000 Hz Nyquist frequency. A 500 Hz high-cut filter with a 24 dB/octave rolloff acted as an anti-alias filter and to reduce high frequency noise. The dynamic range of this floating point seismograph was more than adequate to allow the recording of high-quality reflection information in the presence of source-generated and cultural noise at this site.

Walkaway noise tests were conducted on the northeast end of line 1 (Figure 1). The source (8-gauge auger gun) (Healey et al., 1991) and receivers (three Mark Products L28E 40 Hz) were selected based on field conditions, resolution requirements, target depth, and previous experience. On-site testing concentrated on source/receiver geometries and recording parameters. Test data were recorded with analog low-cut filters out, 50 Hz, 100 Hz, and 200 Hz, station spacing of 8 ft, and source-to-receiver offsets ranging from 8 to 384 ft (Figure 2). The analog filters effectively attenuate ground roll while increasing the dominant frequency of the reflection wavelets (Steeples, 1990). A strong reflection with a zero-offset time of about 140 to 150 msec can be interpreted on all the walkaway files. The calculated NMO velocity is about 2100 ft/sec, which correlates to a depth of around 150 ft (Figure 3). This depth (based on the boreholes near the sinkhole) is about 15% to 20% shallower than expected for the top of the salt and almost double the measured depth to water table. The data quality was sufficient to allow selection of optimum recording parameters and source/receiver geometries targeting reflectors between 50 and 250 ft deep.

Direct waves, refractions, ground roll, reflections, and air-coupled waves can all be identified on the walkaway data (Figure 4). The direct wave possesses a very uniform 1700 ft/sec velocity from the source out to about 300 ft of offset. A refraction arrival is interpretable from about 304 ft to the end of the spread (384 ft), with an apparent linear velocity of around 10,000 ft/sec (this is an unreversed velocity). Two-layer refraction analysis places this first significant acoustic interface at a depth of about 130 to 140 ft. Ground roll velocities range from 800 to 1300 ft/sec. The previously identified 150 msec reflection possesses the greatest potential resolving

power and depth control at near source offsets (i.e., < 200 ft). The prominent reflection may be from the same interface as the refracted waves.

Based on the walkaway data and available equipment, the source-receiver geometry was split-spread with a source-to-nearest-receiver spacing of 12 ft and a furthest offset of 196 ft. The recording parameters included an analog low-cut filter of 50 Hz and a 0.5 msec sampling rate. Identification of coherent arrivals on walk-away data allowed confident selection of parameters and geometries used for the CDP portion of the survey.

The production (CDP) portion of the survey took just over 2 days and included 673 shotpoints of 2-D data along three northwest/southeast lines and one southwest/northeast tie line and a 45 shotpoint 3-D test near the sinkhole at the intersection of lines 2 and 4. The 8-gauge auger gun allowed detonation of a 400 grain black powder load 2 to 3 ft below the ground surface in a water saturated, tightly stemmed 2" hole. The rough wooded terrain, rubble and fill material, shallow tree roots, as well as the narrow paths made the auger gun an ideal source for conditions and required data quality. Three geophones were placed in a 3 ft in-line array at each station to help attenuate source-generated air-coupled waves and other coherent in-line noise. The source was detonated and receivers were planted into competent material beneath the organic surface layer. The seismograph was configured to focus on reflections within the upper 250 msec possessing average velocities from 1200 to 6000 ft/sec. The analog amplitude/frequency spectrum was shaped with 50 Hz analog low-cut filters to enhance and balance the higher frequency components of the reflection energy. This emphasis on spectral shaping was necessary to maximize the chances of separating the water table reflection from the top of the salt and any continuous reflectors between water table and the top of salt.

Data Processing

Data processing was done on an Intel 80486-based microcomputer using *Eavesdropper*, a set of commercially available algorithms. The processing flow was similar to those used in petroleum exploration (Table 1). The main distinctions relate to the conservative use and application of correlation statics, precision required during velocity and spectral analysis, and the accuracy of muting operations. A very low percentage allowable NMO stretch (< 20%) was extremely critical in reducing contributions of shallow reflected energy significantly beyond the critical angle, maximizing resolution potential, and avoiding distortion in the stacked

wavelets (Miller, 1992). Many processing techniques not routinely effective on shallow data sets (including f-k migration, deconvolution, and f-k filtering) were tested to evaluate their potential on this data set. Due to a lack of reflection information shallower than the prominent reflection arrival (Figure 5), data processing beyond brute stack focused on enhancing events deeper than 50 msec.

For most basic shallow high-resolution seismic reflection data the processing steps/operations are a simple scaling down of established petroleum-based processing techniques and methods. However, processes such as deconvolution (especially spiking) have basic assumptions (Yilmaz, 1987) that are violated by most shallow data sets, this data set being no exception. Migration is another operation that, due to non-conventional scaling (vertical and/or horizontal), many times may appear to be necessary when in actuality geometric distortion may be simple scale exaggeration (Black et al., 1994). Migration for this data set was effective in reducing the apparent distortion associated with the subsidence and effectively focusing interpreted reflections. Processing/processes used on data for this report has/have been carefully executed with no *a priori* assumptions and with care not to create anything through processing, but to simply enhance what can be identified on unstacked data.

Datum corrections and time/depth conversions were based on stacking velocities. In the absence of sonic logs and/or checkshot surveys, depth estimations using stacking velocities, estimated arrival times, and multiple sloping datums represents the most accurate method. As many as five sloping datums per line were used to minimize the effects of topography on velocity and static analysis (Figures 6A through 9A). After generation of final stacked sections, data were corrected to a conventional flat datum of 48 ft sea level elevation (Figures 6B through 9B) and were then time/depth converted using the same stacking velocities (Figures 6E through 9E). An adjustment was made to the stacking velocities on lines 1, 2, and 3, to compensate for surface dip. This adjustment is similar in nature to DMO and effectively decreased stacking velocities by less than 10% (Table 3). The result of this topographic velocity adjustment is a perfect tie at the intersection points of all four lines. The elevation corrections and velocity adjustments are site specific and were necessary to accurately represent the geometry of reflecting events.

The experimental 3-D reflection array was collected at the intersection of lines 2 and 4. This data set possesses one-fold redundancy and was processed using parameters established through analysis of 2-D data from line 2 and line 4. The data have been filtered, scaled, muted (based on source offset), elevation corrected,

deconvolved, sorted (binned), NMO corrected, and displayed. The software used was a special set of algorithms developed for the PC in association with *Eavesdropper*.

Results

Unequivocal identification of reflection energy on field files is essential for accurate interpretation of CDP stacked sections. Raw field files acquired during the production portion of the survey from each line have reflection events identifiable between 70 and 150 msec (Figure 5A). The reflections have an average dominant frequency of approximately 80 Hz and an apparent NMO velocity ranging from 1350 to 2100 ft/sec. Approximate depth to the primary reflector was between 50 and 150 ft on most field files (most of the apparent change in depth is a direct result of the more than 70 ft change in surface elevation across the line). The signal-to-noise ratio on the raw field files is very good and allows confident identification of reflections on 90% of the raw field files.

Digital filtering, first-arrival muting, appropriate trace balancing, bad-trace editing, and conservative application of correlation statics were key processes in improving the pre-stack appearance of coherent events interpretable on raw field files (Figure 5B). The coherent event identifiable on filtered and scaled files possesses an arrival pattern consistent with the classic hyperbolic moveout of a reflection. The digital filter applied to this field file narrowed the bandwidth enough to produce a very cyclic or ringy wavelet. Even with the interpretation confidence allowed by these high quality field files, it is still prudent to practice care and a conservative approach to interpretations of coherent energy on stacked data (Steeples and Miller, 1990).

A strong coherent event can be interpreted across all the nominal 24-fold CDP stacked sections (Figures 6 through 9). The irregularity of the reflection over parts of each line is suggestive of either a highly variable (dissolved/faulted and folded) surface or significant velocity variation in the near surface. From analysis of field files, very little variation in velocity of direct, refracted, or reflected waves is observed within the length of a spread. However, across the expanse of some lines the near-surface velocity changes by as much as 30%. The single strong reflection event ties extremely well line-to-line both before and after correction to a flat datum.

The reflection wavelet characteristics are relatively consistent on all four stacked sections. The very high amplitude of the reflection suggests the interface

responsible for this event possesses a high acoustic impedance contrast. From drill data, the velocity at the water table interface changes from around 1800 ft/sec to over 5000 ft/sec, therefore energy incident to the water table interface at angles greater than about 20° will result in nearly total reflectance. Classically, the water table interface, in an unconsolidated (alluvial/colluvial) setting, is a high acoustic contrast (Merey et al., 1992; Hunter et al., 1984). At this site no salt reflections will be recorded at receiver offsets greater than about 140 ft.

The prominent reflection event identified on field files is interpretable across the expanse of lines 1, 2, 3, and 4 (Figures 6A through 9A). The reflection event is coherent and well defined north of about Morton Road but displays a decreased signal-to-noise ratio and reflection wavelet bandwidth to the south (Figure 6A). The dominant frequency drops from about 80 Hz on the north to 50 Hz on the south. The near-surface velocity ranges from 1700 ft/sec on the north to less than 1250 ft/sec on the south, while the stacking velocity ranges from 2000 ft/sec on the north, 1900 ft/sec in the center, and back to over 2100 ft/sec on the south (Table 2). These changes in velocity do not seem to correlate to bandwidth but are consistent with the variability in surface material and elevation across the line.

Indications of a disturbed reflecting surface at several places along line 1 are prevalent (Figure 6D). An apparent disturbance at about CDP 120 is coincident with a 10 to 12 ft deep ditch observed at the ground surface. At best, the ditch could be partially responsible for a very localized portion of this static shift if inaccurate elevation and/or velocity corrections were made during processing. The surface ditch might also somehow be the effect of previous subsurface activity. With the apparent uniformity of the upthrown and downthrown sides and the very localized nature of this "offset zone" it is unlikely the 20 msec offset is due solely to static or velocity problems. South of CDP 190 data quality drops drastically. The reflection event is confidently interpretable out to about CDP 300, but beyond that point the very periodic nature of the energy and the lack of a strong reflection wavelet makes interpretation speculative. The northern half of line 1 clearly suggests an irregular reflecting surface.

General wavelet characteristics, irregularity in the reflecting surface, apparent change in spectral properties, and a drop in signal-to-noise ratio on the southern end of line 2 are consistent with observations of line 1 (Figure 7A). The severe surface topography at the start of line 2 inhibited the acquisition of high fold data between CDP 0 and about 40. The surface of the shallowest reflection on the north

end of the line is very irregular and similar to the character in the northern end of line 1. The surface of the reflector on the south seems to be much smoother with less abrupt changes than on the north.

Line 2 passes within about 50 ft of the eastern edge of the sinkhole. There seems to be no significant disturbance in the reflection that can be attributed to subsidence over the portion of the line adjacent to the sinkhole. The shallowest reflection interpreted north of the intersection of lines 2 and 4 appears disturbed from the southern road ditch to about CDP 125 (Figure 7B). CDP 125 is in about the middle of the wooded area between Morton Road and Snyder Road. The flat datum corrected sections should be free of topographic effect (Figures 7B, 7C, and 7D). The offset north of the intersection of lines 2 and 4 is the most pronounced feature on the section. Based on the general appearance of the stacked section from line 2, the only interpreted feature that could be related to the sinkhole is between CDP 125 and CDP 185.

The stacked section from line 3 has several localized features suggestive of significant offset or irregularities in the surface of the reflection (Figure 8A). An apparent offset in the reflector at CDP 125 is pronounced on data processed with sloping datums. This feature does not correlate to any surface expression or apparent change in near-surface acoustic properties (based on field file analysis). From the northern end of the line to about CDP 185 the shallowest reflection possesses a distinct or focused appearance. In general line 3 is very similar in appearance to the other north/south lines. As with the other north/south lines, the distinct change in data characteristics about midway through the line could be suggestive of either changes in the reflecting interface or changes in material between the reflector and the ground surface.

The distinct offsets at CDP 60 and CDP 125, as well as the change in wavelet characteristics at CDP 185, represent the most significant features on line 3 (Figure 8B). On these data the apparent offsets in the reflecting surface are very localized with no apparent associated energy scatter (Figure 8B). After topographic correction, both offset features are still very pronounced and not likely related to near-surface anomalies. Adjustments for surface terrain altered the apparent dip of the reflection. Based on the general appearance of the reflection, the offset features interpreted on the north half of line 3 are not likely the effects of recent dissolution. These offset features may relate to lineament and shear zones previously suggested, from remote sensing methods, to be present on Weeks Island (Martinez et al., 1976).

The uniformity in the near-surface material and the lack of significant elevation variation across line 4 was key to the wavelet consistency on this stacked section (Figure 9A). With the dominant stacked reflection frequency about 80 Hz and an approximate average velocity of 1500 ft/sec, the vertical resolution based on 1/4 wavelength criteria of Widess (1973) is approximately 5 ft and the radius of the first Fresnel zone is about 25 ft. The most striking feature on this line is the depression between CDP 180 and 210. This feature is directly adjacent to the sinkhole. Based on the stacking velocities, the depth to the shallowest reflecting interface on the edge of the disturbed zone is about 80 ft. The depth of the depression, as interpreted from the seismic data, is about 15 ft. Due to edge effects it is unlikely that the vertical extent of the depression could be fully resolved with these data.

The apparent depth of the reflector changes slightly across line 4. With lower stacking velocity on the east end of the line, the calculated depth to the reflector is relatively consistent at between 75 and 80 ft between CDP 10 and CDP 180. The increase in stacking velocity from about CDP 250 to the west end of the line corresponds to an increase in depth to the reflector on the west (CDP 260 = 94 ft; CDP 250 = 110 ft). Acquisition limitations at the intersection of Advanced Products Road and Morton Road resulted in a significant drop in fold and may be responsible for the slight offset between CDP 275 and CDP 280 (Figure 9B). The only other noteworthy features on line 4 are the changes in reflection wave character observable at CDPs 110, 240, and 310. These are near or over a large area of suspected rubble fill, a culvert and surface drainage channel, and an area with the remains of a structure. These changes in wavelet characteristics are similar to those observed on all three north/south lines. Since line 4 was acquired approximately parallel to the topographic gradient, very little relative change in reflection orientation can be observed after correction to a flat datum (Figure 9B). Based on the stack of line 4, the anomaly observed in the shallowest reflection between CDP 180 and CDP 210 is directly related to the surface subsidence near station 100 (CDP 200).

A variety of signal enhancement processes were evaluated on these data. The primary goal was to determine if any reflection signal deeper than the primary reflection could be enhanced. The effectiveness of second-zero crossing and spiking deconvolution was likely inhibited by violation of two of the three basic premises associated with deconvolution (random time series/large number of unique reflections and high signal-to-noise). Along portions of the CDP stacked sections with high signal-to-noise (S/N) ratios deconvolution did seem to suppress the

reflection wavelet and broaden the bandwidth (Figures 6C through 9C). The application of a constant velocity f-k migration made the most noticeable improvement to the stacked data, especially on line 4 in the area adjacent to the sinkhole (Figures 6D through 9D). Migration only mildly enhanced signal deeper than the prominent reflection. F-k filtering (velocity filter) was no more effective than a simple NMO stretch mute in removing wide-angle reflection energy present on field files, but it did narrow the effective pass band and resulted in a ringy appearance. The improvement observed after f-k filtering was not sufficient to justify the subtle artifacts of the operation. Some of the more sophisticated signal processing operations improved S/N and reduced geometric distortion, allowing more confidence in suggestions that reflections from the salt and a single intermediate layer between the shallowest reflection and the salt may be interpretable.

Interpretations

Time/depth conversion based on the stacking velocity function was performed on each migrated, stacked section (Figures 6E through 9E). The most notable features enhanced by this display are the apparent offset (down to the north) in the high amplitude shallow reflection about mid-way across lines 1, 2, and 3, and the subsurface expression of the sinkhole on line 4. The depth to this shallow reflecting interface on the south end of lines 1, 2, and 3 and the east end of line 4 is consistent with the drill-determined water table. At least two unique reflections besides the proposed water table reflection can be inferred on the three north/south sections. It is possible that the deeper event (around 180 to 200 ft) is the top of salt. The interface responsible for the proposed intermediate reflecting event has not been confidently identified or correlated to any stratigraphic interface.

From VSP data and drill logs, the reflection at about sea level elevation on the south end of lines 1, 2, and 3 and on the east end of line 4 is from the water table. The influence and proximity of the Gulf make sub-sea level water table depths questionable assuming uniform permeability of the local sediments. If the water table reflector is offset by as much as the 50 ft suggested on lines 2 and 3 (Figures 7F and 8F) then either the water table on the south side of the offset is perched, the permeability and porosity north of the offset is significantly less than that on the south, or within the offset zone there is some kind of hydrologic barrier inhibiting horizontal movement. Interpreting the shallowest reflection as the water table

across all lines (Figures 6F through 9F) suggests a major hydrologic gradient and associated linear pressure ridge or transition zone.

If the water table reflector is not present north of the disturbed zone it is likely that faults and/or fractures are acting as conduits for vertical fluid movement (Figures 6G through 9G). Drawdown of the water table may be acoustically represented on line 1 by the apparent localized northward dip between CDPs 200 and 140 and on line 3 by the same northward dip between CDPs 260 and 200. Assuming the apparent abrupt termination and drawdown in the water table reflection along a lineament intersecting CDP 140 on line 1, CDP 190 on line 2, and CDP 200 on line 3 are accurate interpretations, it is reasonable to suggest this offset hydrologically represents the subsurface analog to a water fall. Two existing surface features could be expressions of this lineament: the present sinkhole and a steep sided ditch approximately 30 ft across and 10 ft deep that intersects line 1 at approximately CDP 120. If the waterfall scenario is accurate, active dissolution and subsidence along this lineament is inevitable with the rate and location of dissolution and the resulting subsidence controlled at least in part by permeability and soil properties.

The two reflections interpretable on lines 1, 2, and 3 below sea level are relatively flat provided the water table reflector terminates mid-way across the survey line (Figures 6G through 9G). With the extreme acoustic contrast between the near-surface material at around 1700 ft/sec and the first significant velocity change to around 6000 to 7000 ft/sec (whether it be water table or a clay/shale) the shallowest reflection arrival will always possess a relative high amplitude at this site. Therefore wavelet similarities in the shallowest recorded reflection event across the lines do not necessarily constitute reflector consistency. The deepest event interpretable on the sections, at about -150 ft elevation, seems to possess a substantially lower dominant frequency. The approximate depth and wavelet characteristics of this event are consistent with previous interpretations of the top of salt (*Leading Edge,* August 1994 issue). The reflection event interpreted at about -50 ft elevation may be the same event acoustically imaged in this area and tentatively identified as a shale layer (Kinsland and Rutter, 1994). The undulating surface of the reflection at -50 ft elevation is suggestive of paleo-subsidence topography.

The drop in resolving power and general data quality on the southern half of the three north/south lines and along portions of the east/west line (Figures 6A through 9A) correspond to a single lineament that traverses the entire survey area approximately parallel to Morton Road (Figure 10). Regardless of the continuity or

lack of continuity of the water table reflection, the data quality, reflection signature, and depth to shallowest reflection dramatically changes at this lineament. The sinkhole seems to lie along the northern edge of this lineament (maybe a shear zone). Long linear features have been suggested previously on Weeks Island (Martinez et al., 1976). Some of these long linear features align with shear zones associated with the flanks of the dome. Water seeps, vertical chimneys, and highly folded black salt identified within the mine prior to its use as a petroleum storage facility are suggestive of shear zone boundaries (Martinez et al., 1977). The distinct change in wavelet characteristics on the seismic data and the termination or offset in the water table reflection, in general, does not contradict previously suggested shear zones along the edge of the mineworks.

3-D Results

Forty-five shotpoints of one-fold 3-D data were acquired at the intersection of lines 2 and 4 (Figure 1). The data for the 3-D survey were acquired coincident with the acquisition of line 4. During the process of rolling through the 2-D line (line 4), acquisition was halted when the spread was equally split by line 2. At that point the source was moved 24 stations off-line to the north along line 2. Maintaining a fixed spread, the source was walked south along line 2, crossing Morton Road and line 4 until 24 shotpoints south of line 4 had been recorded. The survey effectively consisted of a fixed 48-channel, 376 ft split-spread source/receiver geometry between stations 66 and 113 on line 4 with 45 unique off-line offsets, each separated by 8 ft and starting 188 ft north of the intersection of lines 2 and 4 and ending 188 ft south of that intersection. The surface configuration of this one-fold survey was a 90-degree cross with the 45 shotpoints along one arm and the 48 receivers along the other.

The 3-D data quality (i.e., signal-to-noise) was sufficiently high to allow an interpretation when displayed in a volumetric wiggle-trace diagram (Figure 11). The processing parameters were determined using the analysis already completed for lines 2 and 4. The lack of redundancy would have inhibited accurate processing of the 3-D data without the 2-D data. The resulting data clearly show the depression on the surface of the prominent reflector identified on the high-fold 2-D lines.

Conclusions

The subsurface expression of the sinkhole was effectively imaged with shallow seismic reflection techniques. The effects of dissolution and the resulting subsidence that produced the Weeks Island sinkhole have a distinctive acoustic expression on multi-fold 2-D and single-fold 3-D. Both interpretations of the 2-D data suggest an active hydrologic setting with continued subsidence likely along a northeast/southwest lineament.

The coherent reflection event interpretable on all four lines is dramatically altered on line 4 adjacent to the sinkhole. Line 2 possesses a depression in the reflection consistent in depth with line 4 but not as dramatic. The drill data suggest the depression in the reflection on line 4 near the sinkhole is a drawdown in the water table similar to drawdown experienced during classic pumping tests. The depression imaged by line 2 is either a subsurface subsidence without surface expression or an irregular surface not directly related or hydraulically connected to the present sinkhole or active subsidence. From the seismic section along line 4 the subsurface expression of the sinkhole is very steep and probably best described as a chimney feature.

The shallowest reflection in close proximity to the sinkhole was drill confirmed to be water table. The offset in the shallowest reflection is suggestive of a severe hydrologic pressure gradient across a distance of less than 100 ft and a subsea level water table less than a mile from the Gulf (Figure 10). The high amplitude nature of the shallowest reflection is related to acoustic contrast and not necessarily a criterion for reflector continuity.

Correlation of the sinkhole with the edge of the mined area and the seismically inferred lineament is probably more than a coincidence. The previously suggested shear zone that marks the southern edge of the mine could be represented acoustically by a localized change in signal characteristics or discontinuities in reflecting interfaces. It is likely that future dissolution and associated subsidence in the area examined with shallow reflection will be concentrated along this lineament.

Recommendations

The data presented and interpreted here needs more ground truth (i.e., several checkshot velocity surveys). These data have undergone CDP processing without incorporation of other geologic or geophysical data. The velocity, and

therefore depths, are based on curve matching techniques that could possess as much as 20% error (Hughes, 1985). With the extreme variation in velocity across this site and with the need for a high level of depth accuracy, stacking velocities need to be replaced with true average velocities for depth calculations.

The area suggested in this report as susceptible to subsidence needs confirmation drilling. A drill hole at least 400 ft north of the lineament (between stations 30 and 40 on lines 1, 2, and 3) is critical to determine the interface responsible for the reflection at -50 ft. A drill hole placed at approximately station 85 on line 2 would determine if the disturbed reflecting surface identified on line 2 and speculated to be related to the sinkhole was truly an extension of the subsidence feature identified on line 4 or the result of uplift or previous dissolution. If drilling encounters a void or any indication of active subsidence, a second drill hole should be attempted near station 60 to determine northern extent. If no void is encountered, the disturbed surface probably should not be considered an immediate threat.

The 3-D test survey clearly shows the utility of the method in this area when incorporated into a thorough 2-D program. A more extensive survey, possibly including multi-fold 3-D data, would be an effective method to improve the accuracy of the interpretation of this feature as well as delineate other potential subsidence features as directed by these and future 2-D lines. It is clear from this study that in this area 3-D data can be most efficiently be used when acquired coincident with 2-D. The 3-D data acquired as a test on this survey could undergo more extensive processing. However, the gain versus cost might not be justified. The velocity variation observed across the area included with this 3-D survey suggests conventional 3-D velocity analysis and possibly migration should improve the accuracy of future 3-D surveys.

References

Black, W.E. and J.O. Voigt, 1982, The use of seismic refraction and mine-to-surface shooting to delineate salt dome configuration and map fracture zones [Exp. Abs.]: Soc. Explor. Geophys., p. 465-466.

Black, R.A., D.W. Steeples, and R.D. Miller, 1994, Migration of shallow seismic reflection data: *Geophysics,* v. 59, p. 402-410.

Healey, J., J. Anderson, R.D. Miller, D. Keiswetter, D.W. Steeples, and B. Bennett, 1991, Improved shallow seismic-reflection source: Building a better Buffalo [Exp. Abs.]: Soc. Explor. Geophys. v. 1, p. 588-591.

Hughes, D.R., 1985, Velocity without tears: *The Leading Edge,* v. 4, n. 2, p. 50-52.

Hunter, J.A., S.E. Pullan, R.A. Burns, R.M. Gagne, and R.S. Good, 1984, Shallow seismic-reflection mapping of the overburden-bedrock interface with the engineering seismograph–Some simple techniques: *Geophysics*, v. 49, p. 1381-1385.

Kinsland, G.L. and A.W. Rutter, III, 1994, Shallow seismic survey on Weeks Island, Louisiana, ... an attempt to define "top of salt," submitted to Gulf Coast Association of Geological Societies.

The Leading Edge, 1994, Special issue on subsalt imaging: Soc. Explor. Geophys. v. 13, n. 8, August.

Martinez, J.D., et al., 1976, An investigation of the utility of gulf coast salt domes for the storage or disposal of radioactive wastes: Office of Waste Isolation, Union Carbide Corporation–Nuclear Division, U.S. Energy Research and Development Administration. Report ORNL-Sub-4112-25 prepared by the Institute for Environmental Studies, Louisiana State University.

Martinez, J.D., et al., 1977, An investigation of the utility of gulf coast salt domes for the storage or disposal of radioactive wastes: Office of Waste Isolation, Union Carbide Corporation–Nuclear Division, U.S. Energy Research and Development Administration. Report Y/OWI/SUB-4112/37 prepared by the Institute for Environmental Studies, Louisiana State University.

Merey, C. R.D. Miller, E.J. Ticken, and J.S. Lewis, 1992, Hydrogeologic characterization using a shallow seismic reflection survey at Fort Ord, California [Exp. Abs.]: Soc. Explor. Geophys., v. 1, p. 370-373.

Miller, R.D., 1992, Normal moveout stretch mute on shallow-reflection data: *Geophysics*, v. 57, p. 1502-1507.

Miller, R.D., D.W. Steeples, L. Schulte and J. Davenport, 1993, Shallow seismic-reflection feasibility study of the salt dissolution well field at North American Salt Company's Hutchinson, Kansas, facility: *Mining Engineering*, October, p. 1291-1296.

Steeples, D.W., 1990, Spectral shaping during acquisition of seismic-reflection data [Exp. Abs.]: Society of Explor. Geophys., v. 1, p. 917-920.

Steeples, D.W., R.W. Knapp, and C.D. McElwee, 1986, Seismic reflection investigations of sinkholes beneath Interstate Highway 70 in Kansas: *Geophysics*, v. 51, p. 295-301.

Steeples, D.W., and R.D. Miller, 1987, Direct detection of shallow subsurface voids using high-resolution reflection techniques; *in* Sinkholes: Their geology, engineering, and environmental impact, 2nd edition., ed. Barry Beck and W.L. Wilson: A.A. Balkema, Boston, p. 179-183.

Steeples, D.W., and R.D. Miller, 1990, Seismic-reflection methods applied to engineering, environmental, and ground-water problems: Soc. Explor. Geophys. Investigations in Geophysics, Investigations in Geophysics no. 5, Stan Ward, ed., *Volume 1: Review and Tutorial,* p. 1-30.

Widess, M.D., 1973, How thin is a thin bed?: *Geophysics*, v. 38, p. 1176-1180.

Yilmaz, O., 1987, Seismic data processing; S. M. Doherty, Ed.; *in* Series: Investigations in Geophysics, no. 2, Edwin B. Neitzel, Series Ed.: Soc. of Explor. Geophys., Tulsa, Oklahoma.

TABLE 1

Processing Flow

Primary Processing
format from SEG2 to KGSEGY
preliminary editing (automatic bad trace edit with 10 msec noise window)
trace balancing (150 msec window)
first arrival muting (direct wave and refraction)
surgical muting (removal of groundroll based on trace-by-trace arrival)
assign geometries (input source and receiver locations)
elevation correction to multiple, floating datums
sort into CDPs (re-order traces in common midpoints)
velocity analysis (whole data set analysis on 100 ft/sec increments)
spectral analysis (frequency vs amplitude plots)
NMO correction (station dependent ranging from 1350 to 2,500 ft/sec)
correlation statics (2 msec max shift, 7 pilot traces, 100 msec window)
digital filtering (bandpass 25-50 250-375)
secondary editing (manual review and removal of bad or noisy traces)
CDP stack
amplitude normalization (whole trace with 40 msec delay)
correct to flat datum (48 ft above sea level)
display

Secondary Processing
f-k filtering
f-k migration
deconvolution (spiking and second zero crossing)

Table 1. Processing flow for CDP stacked data. Parameters were determined by analysis for each prior step as well as through iterative analysis of particular operations.

TABLE 2

Normal Noveout Velocities, Weeks Island, LA

	CDP#	Time (ms)	Velocity (ft/s)	Time (ms)	Velocity (ft/s)
Line 1 (A)	1	200	2000		
	100	200	1900		
	195	200	1400		
Line 2 (B)	21	200	2000	300	2100
	100	200	2200	300	2300
	200	200	1400	300	1900
Line 3 (C)	150	200	2100	300	2400
	190	200	1700	300	2400
	220	200	1600	300	1900
	250	200	1300	300	2400
Line 4 (D)	10	140	1400	180	2100
	100	140	1400	180	2000
	170	140	1400	180	2000
	200	140	1500	180	1900
	250	140	1700	180	1900

TABLE 3

Velocities Used for Elevation and Depth Calculation

		Datum Correction	Time/Depth Conversion
	CDP #	Velocity (ft/sec)	Velocity (ft/sec)
Line 1	1	2000	1850
	100	1900	1750
	195	1400	1250
Line 2	1	2000	
	21	2000	1850
	100	2200	2050
	195	1400	1250
Line 3	1	2100	1950
	150	2100	1950
	190	1700	1550
	220	1600	1450
	250	1300	1150
Line 4	1	1400	1400
	100	1400	1400
	170	1400	1400
	200	1500	1500
	250	1700	1700

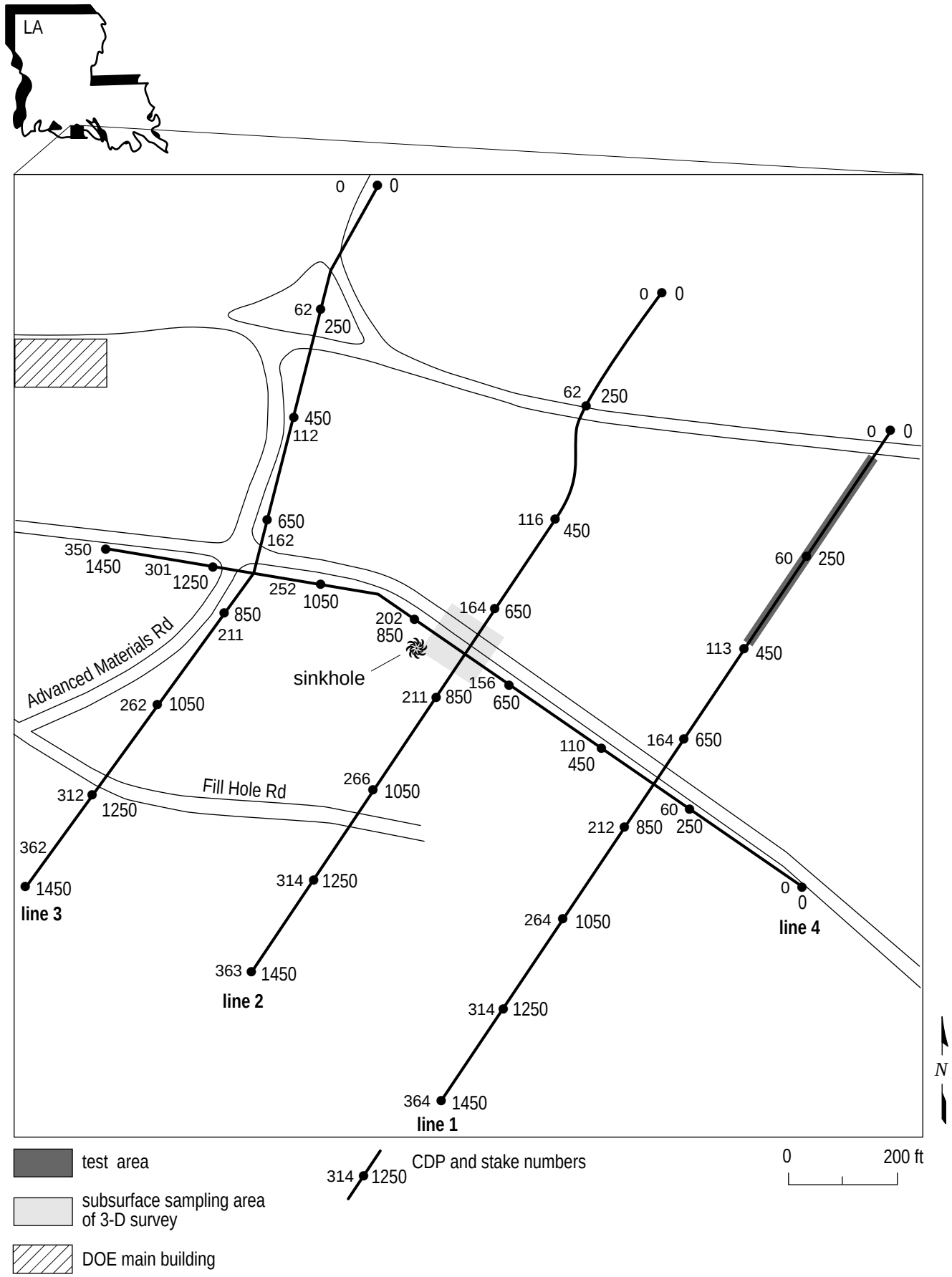

Figure 1. Site map indicating the relative location of Weeks Island and the layout of the survey. The four seismic lines are annotated with both survey distance measurements and CDP numbers. The shaded area represents the subsurface footprint of the 3-D test survey. The walkaway tests were conducted on the northeast end of line 1.

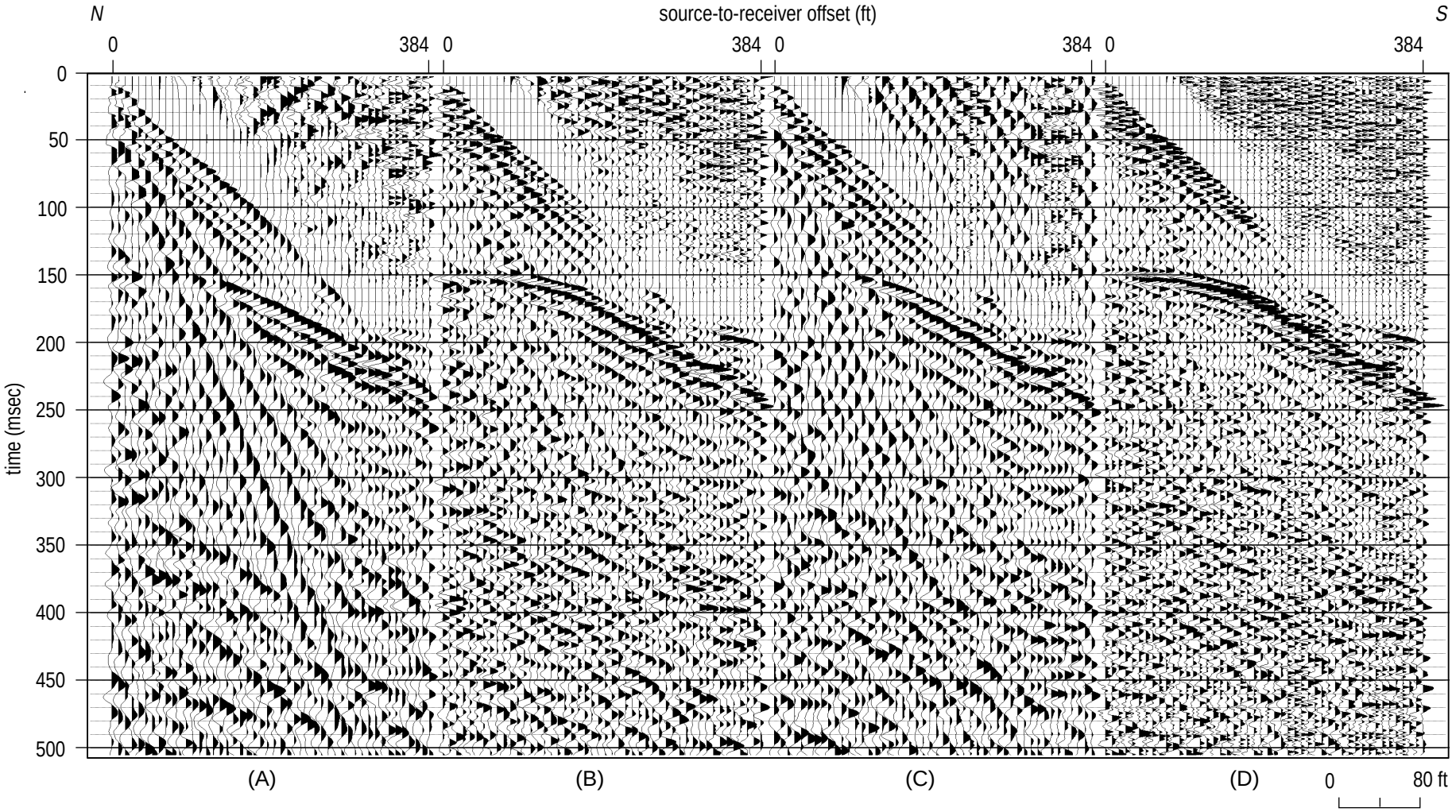

Figure 2. Walkaway noise tests conducted along the northeastern end of line 1. The four files were acquired with the same geophones and source location but different analog low-cut filters (a) out, (b) 100 Hz, (c) 50 Hz, and (d) 200 Hz. The prominent 145 msec reflection possesses textbook curvature and a dominant frequency of over 150 Hz on the 100 Hz low-cut file. Vertical resolution potential is less than 3 ft.

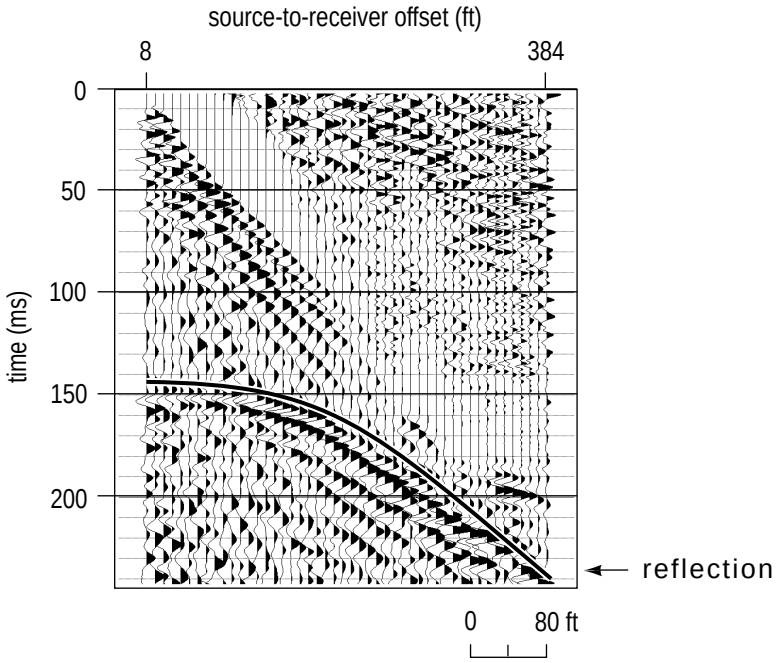

Figure 3. A computer simulated, 2100 ft/sec reflection hyperbola is displayed over field file (b) from the walkaway noise test (Figure 2). The theoretical curve is a perfect match. Depth conversion indicates the reflector is 150 ft deep.

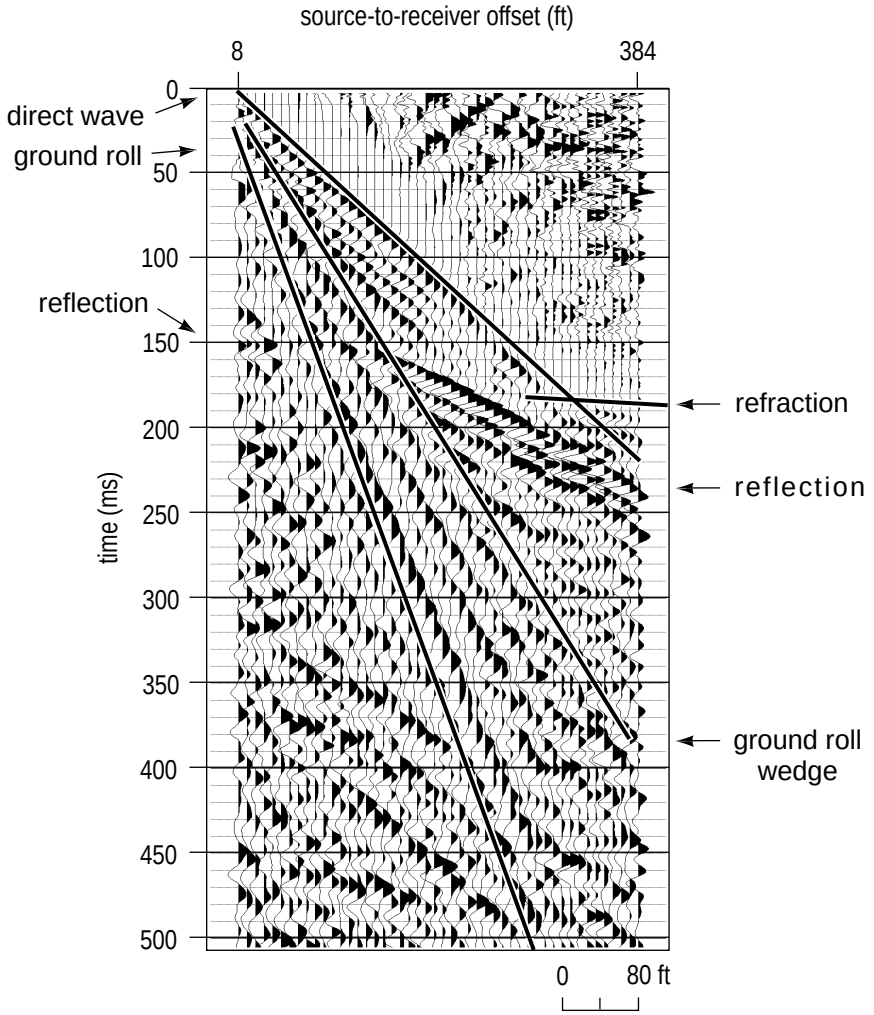

Wave Type	Velocity (ft/sec)	
direct wave	1,700	(linear)
refraction	10,000	(linear)
reflection	2,000	(hyperbolic)
ground roll	800	(linear)

Depth to: reflection ≅ 140, refraction ≅ 130 ft
Refraction depth based on unreversed profile

Figure 4. Walkaway file collected with a 50 Hz analog low-cut filter, then AGC scaled, and highlighted interpretation of coherent arrivals. The analysis suggests the prominent reflection and refraction are from the same interface.

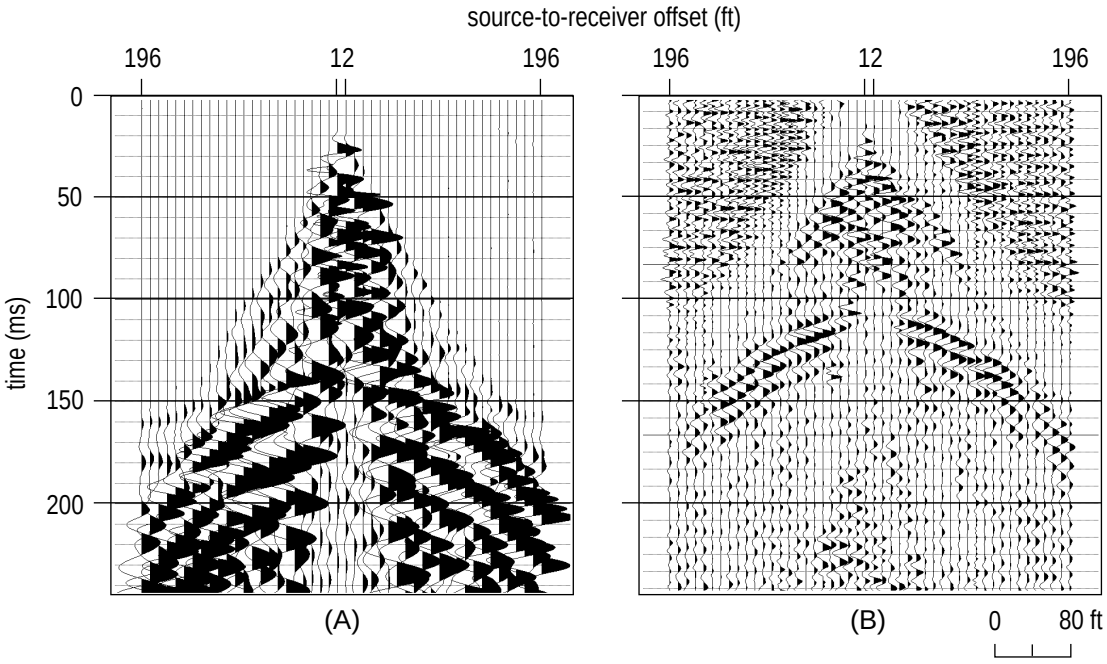

Figure 5. Raw field file (A) and normalized/filtered field file (B) from along line 4. In this split-spread source/receiver geometry the reflection traces a symmetric hyperbola near offset of 12 ft and far offset of 196 ft.

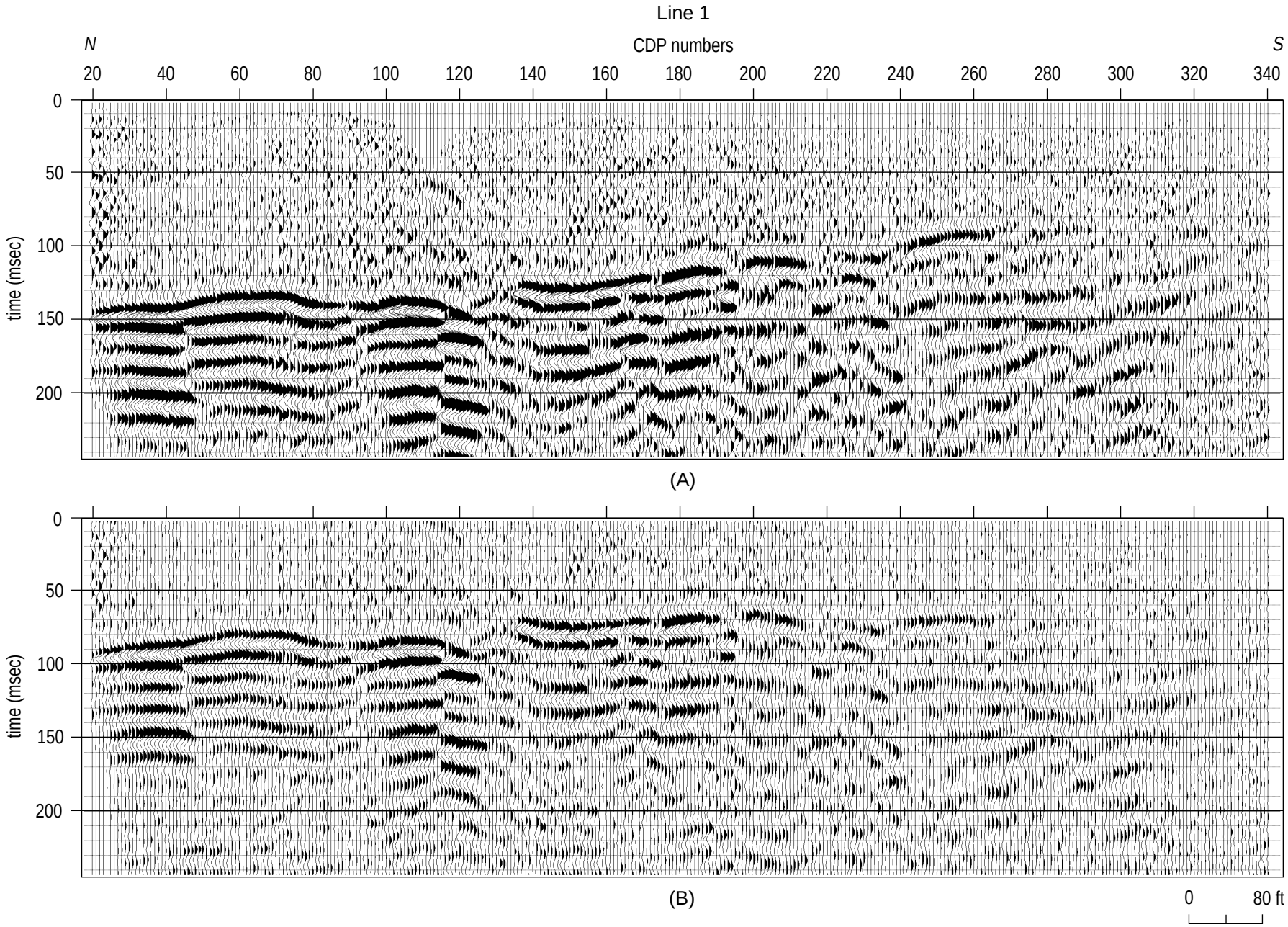
Line 1
N
CDP numbers
S
20
40
60
80
100
120
140
160
180
200
220
240
260
280
300
320
340
0
50
100
150
200
time (msec)
(A)
(B)
0
80 ft

Figure 6A-B.

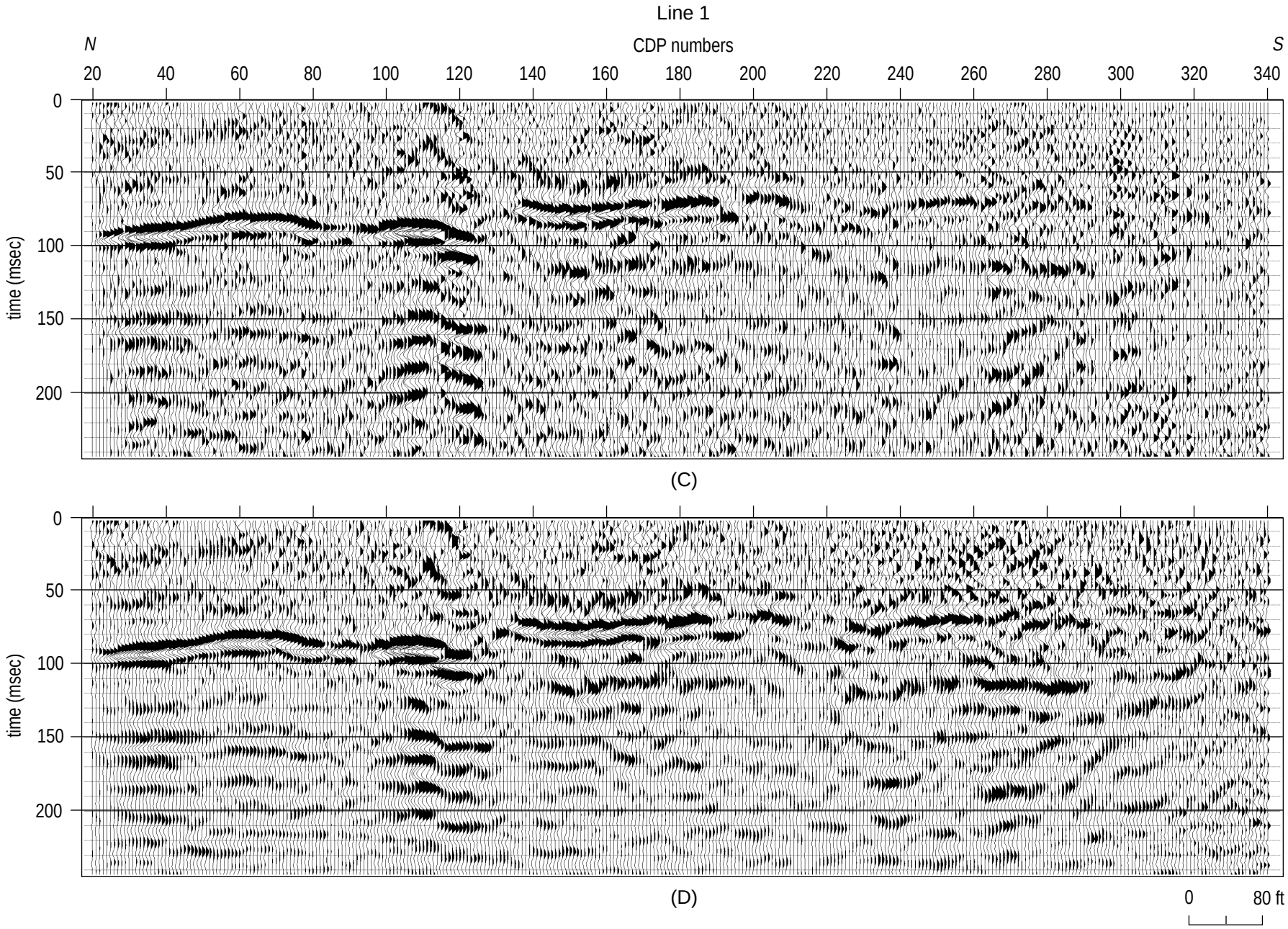
Line 1
N
CDP numbers
S
20
40
60
80
100
120
140
160
180
200
220
240
260
280
300
320
340
0
50
100
150
200
time (msec)
(C)
0
50
100
150
200
time (msec)
(D)
0
80 ft

Figure 6C-D.

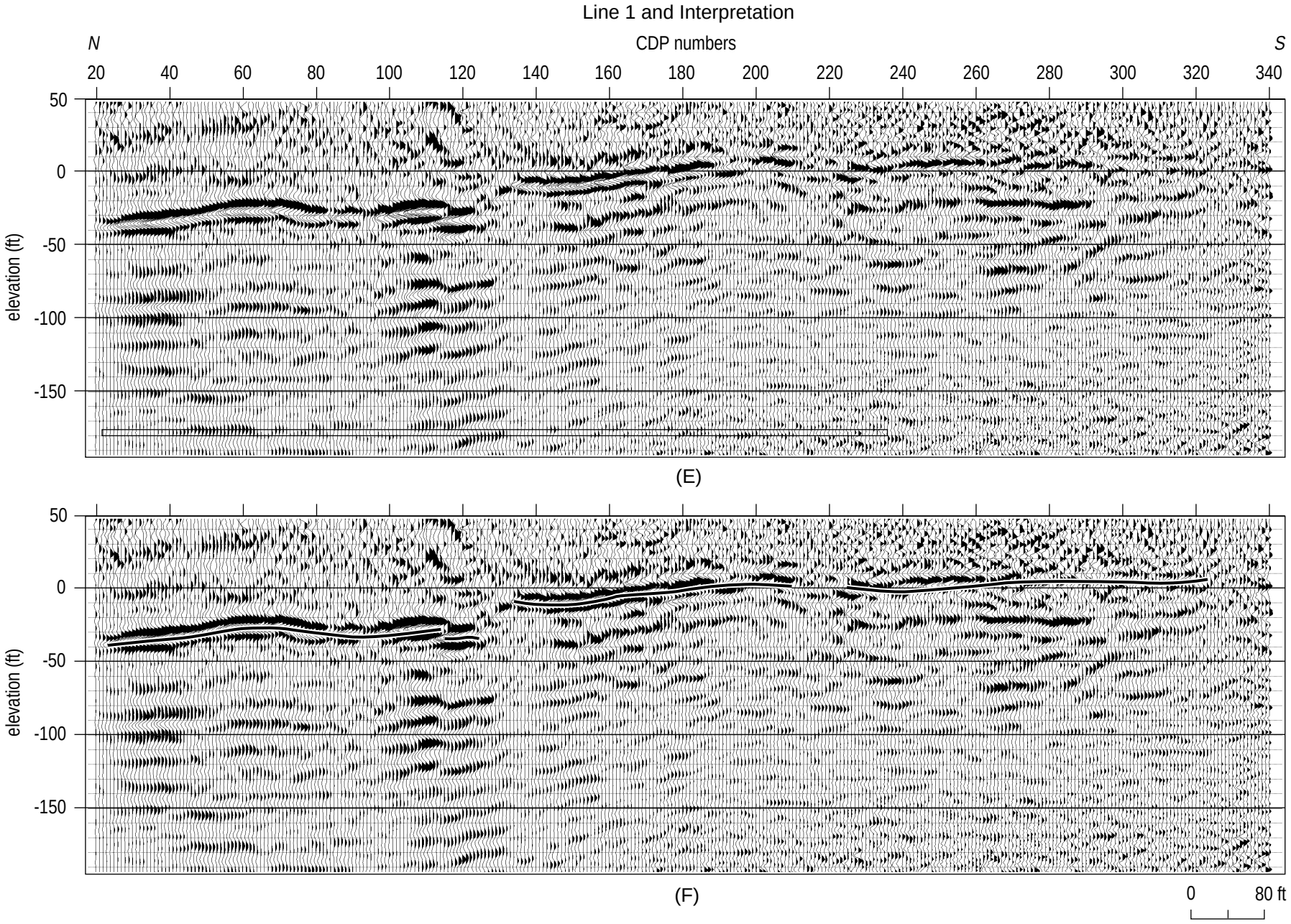
Line 1 and Interpretation
N
CDP numbers
S
20
40
60
80
100
120
140
160
180
200
220
240
260
280
300
320
340
50
0
-50
-100
-150
elevation (ft)
(E)
(F)
0
80 ft

Figure 6E-F.

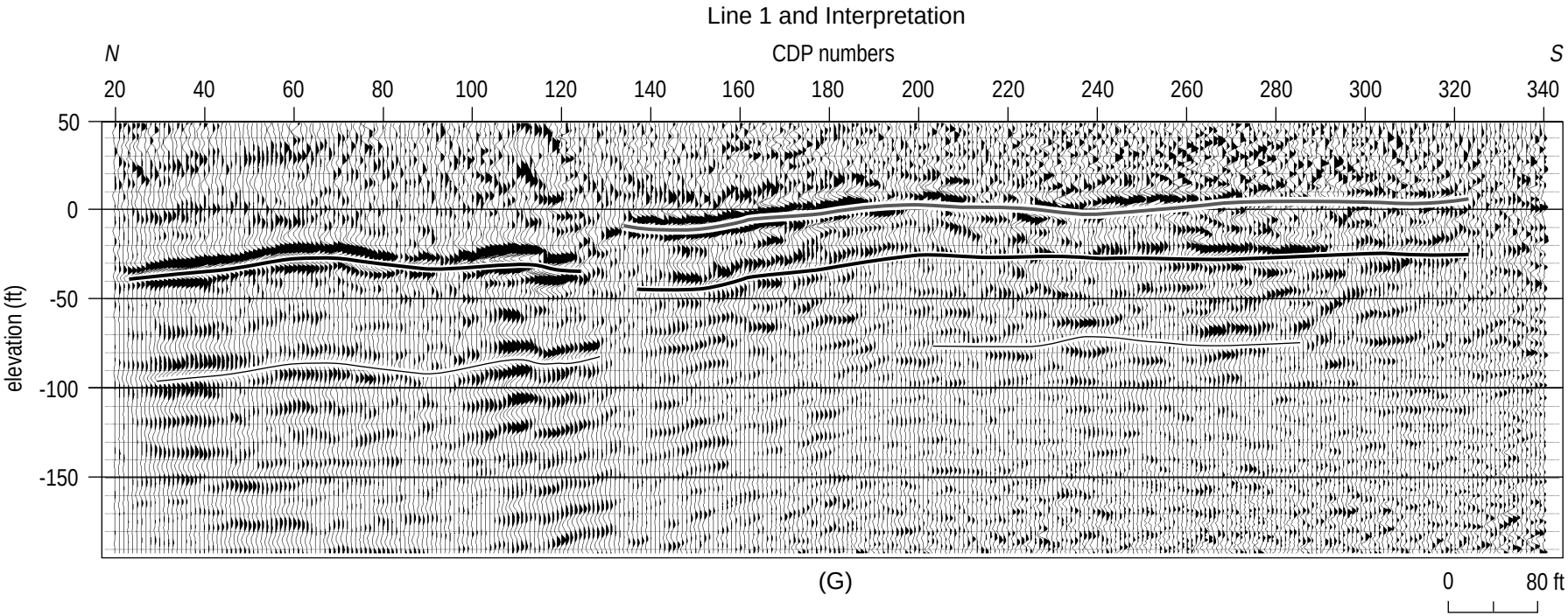

Figure 6A-G. Line 1, 24-fold, CDP stacked section. A) Elevation corrected to multiple sloping datums. B)Same CDP data as (A) elevation corrected to a single flat 48 ft sea level datum. C)Deconvolved (B). D)F-k migrated (C). E)Depth converted (D) using the stacking velocities. F)Interpreted (E) assuming the shallowest reflection is from the same reflector across the line. G)Interpretation of (E) if the shallowest reflection is discontinuous at the apparent offset.

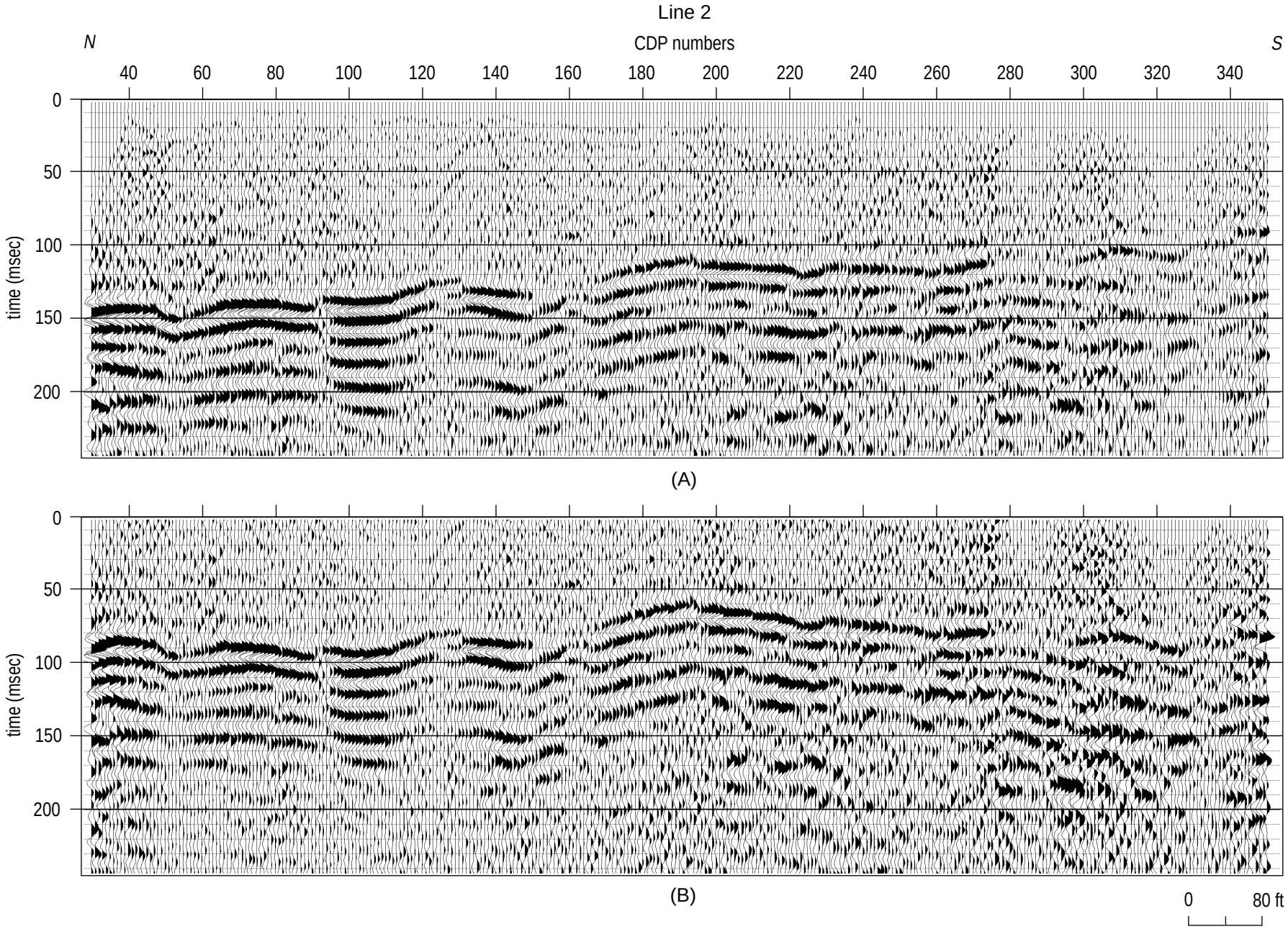
Line 2
N
CDP numbers
S
40
60
80
100
120
140
160
180
200
220
240
260
280
300
320
340
0
50
100
150
200
time (msec)
(A)
(B)
0
80 ft

Figure 7A-B.

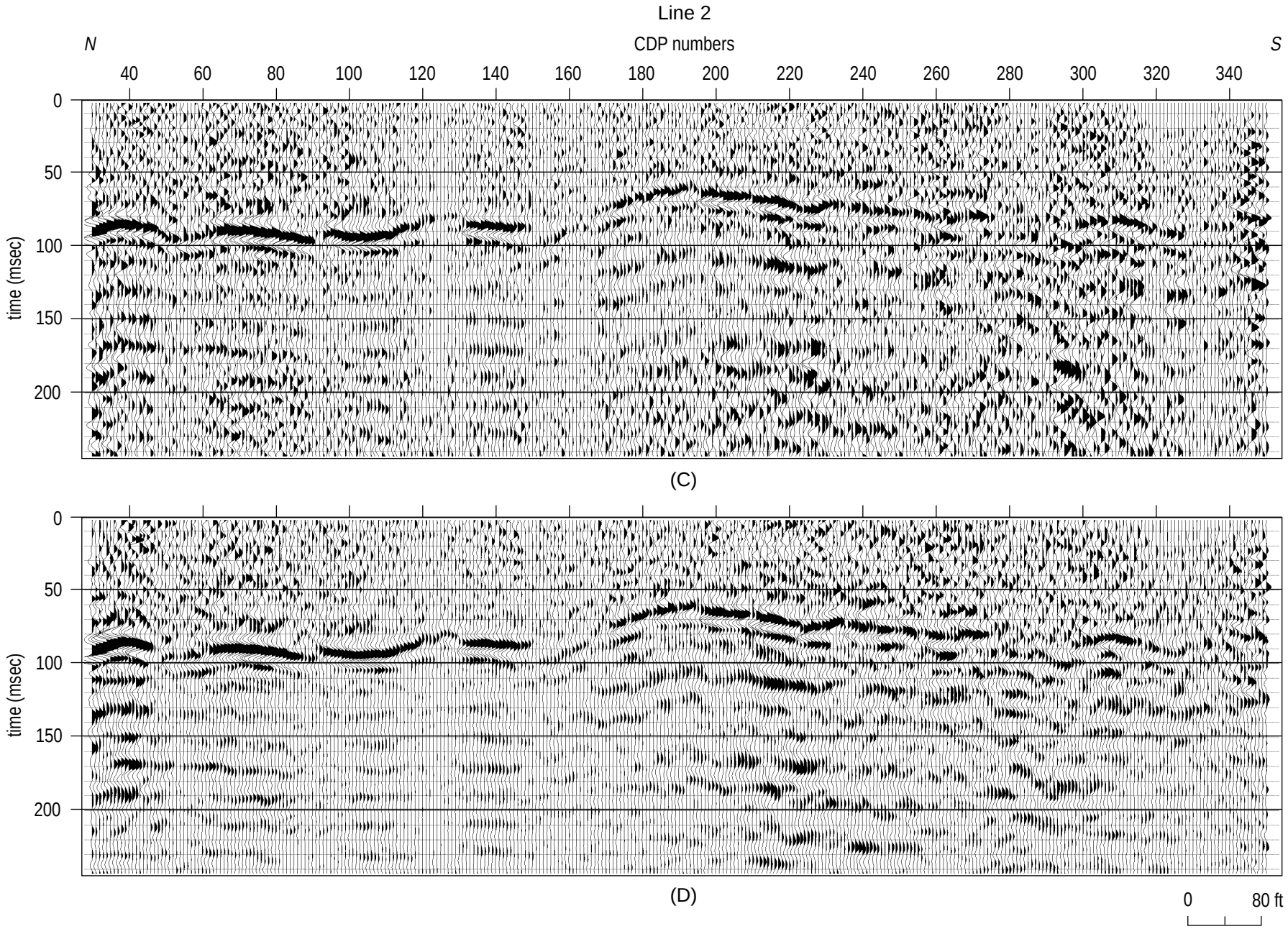
Line 2
N
CDP numbers
S
40
60
80
100
120
140
160
180
200
220
240
260
280
300
320
340
0
50
100
150
200
time (msec)
(C)
(D)
0
80 ft

Figure 7C-D.

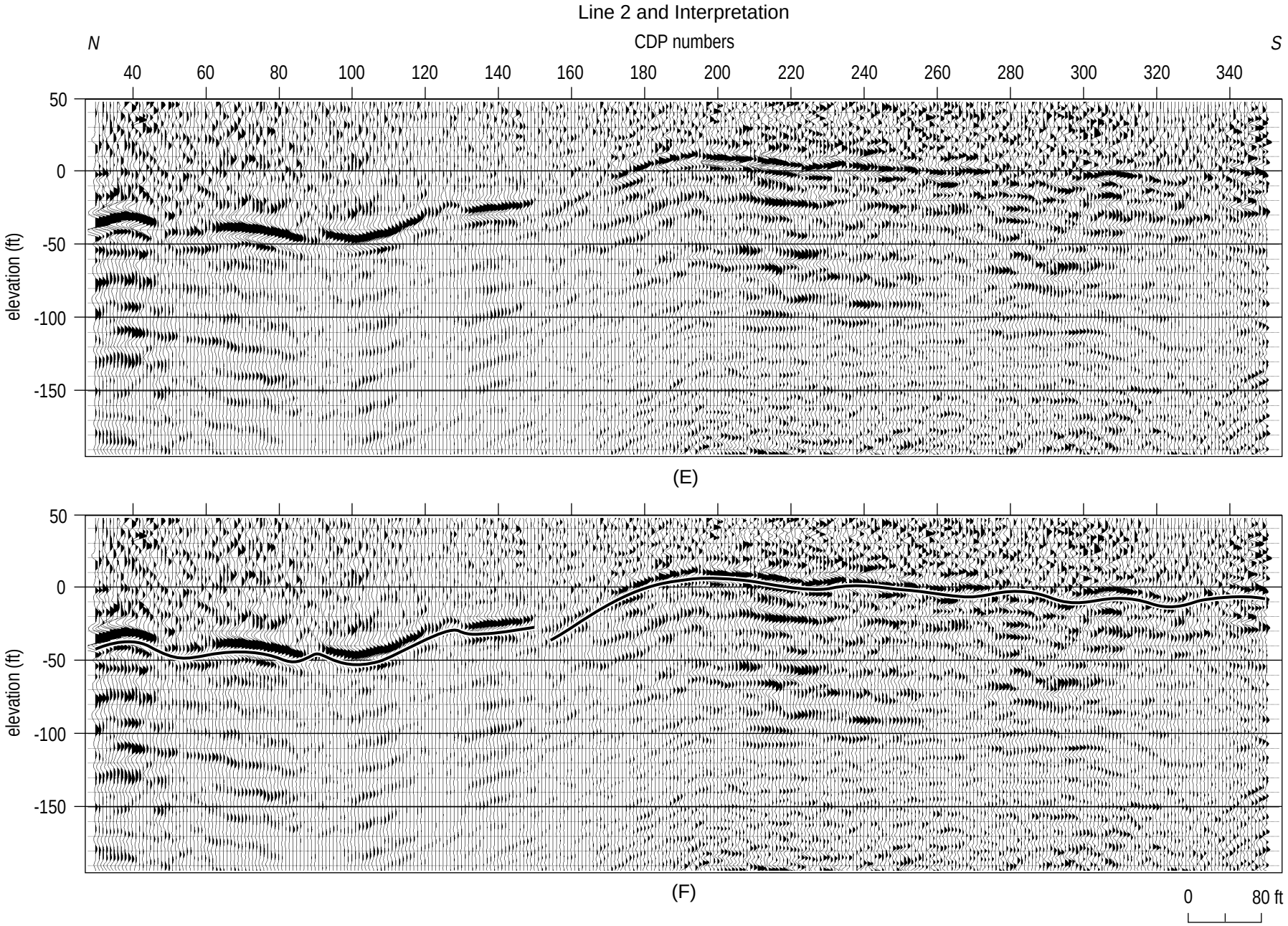
Line 2 and Interpretation
N
CDP numbers
S
40
60
80
100
120
140
160
180
200
220
240
260
280
300
320
340
50
0
-50
-100
-150
elevation (ft)
(E)
50
0
-50
-100
-150
elevation (ft)
(F)
0
80 ft

Figure 7E-F.

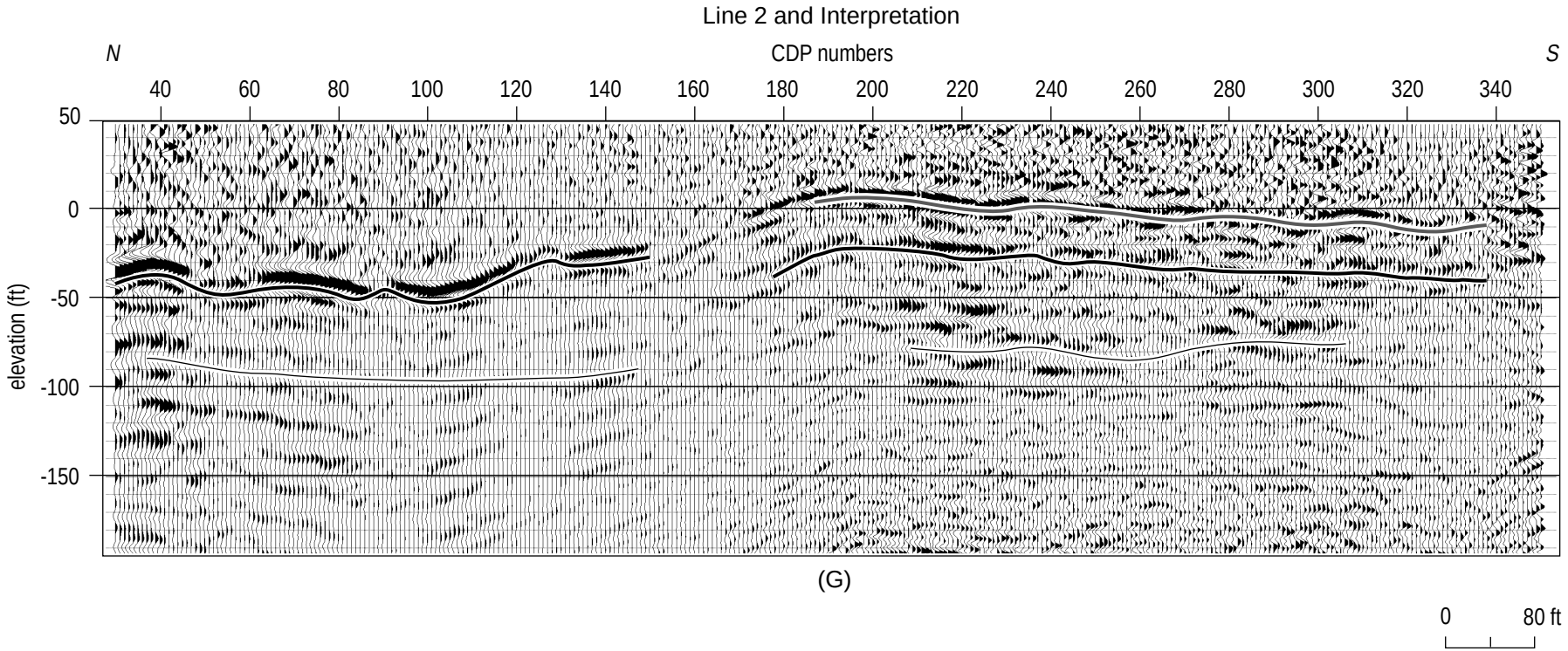

Figure 7A-G. Line 2, 24-fold, CDP stacked section. A) Elevation corrected to multiple sloping datums. B)Same CDP data as (A) elevation corrected to a single flat 48 ft sea level datum. C)Deconvolved (B). D)F-k migrated (C). E)Depth converted (D) using the stacking velocities. F)Interpreted (E) assuming the shallowest reflection is from the same reflector across the line. G)Interpretation of (E) if the shallowest reflection is discontinuous at the apparent offset.

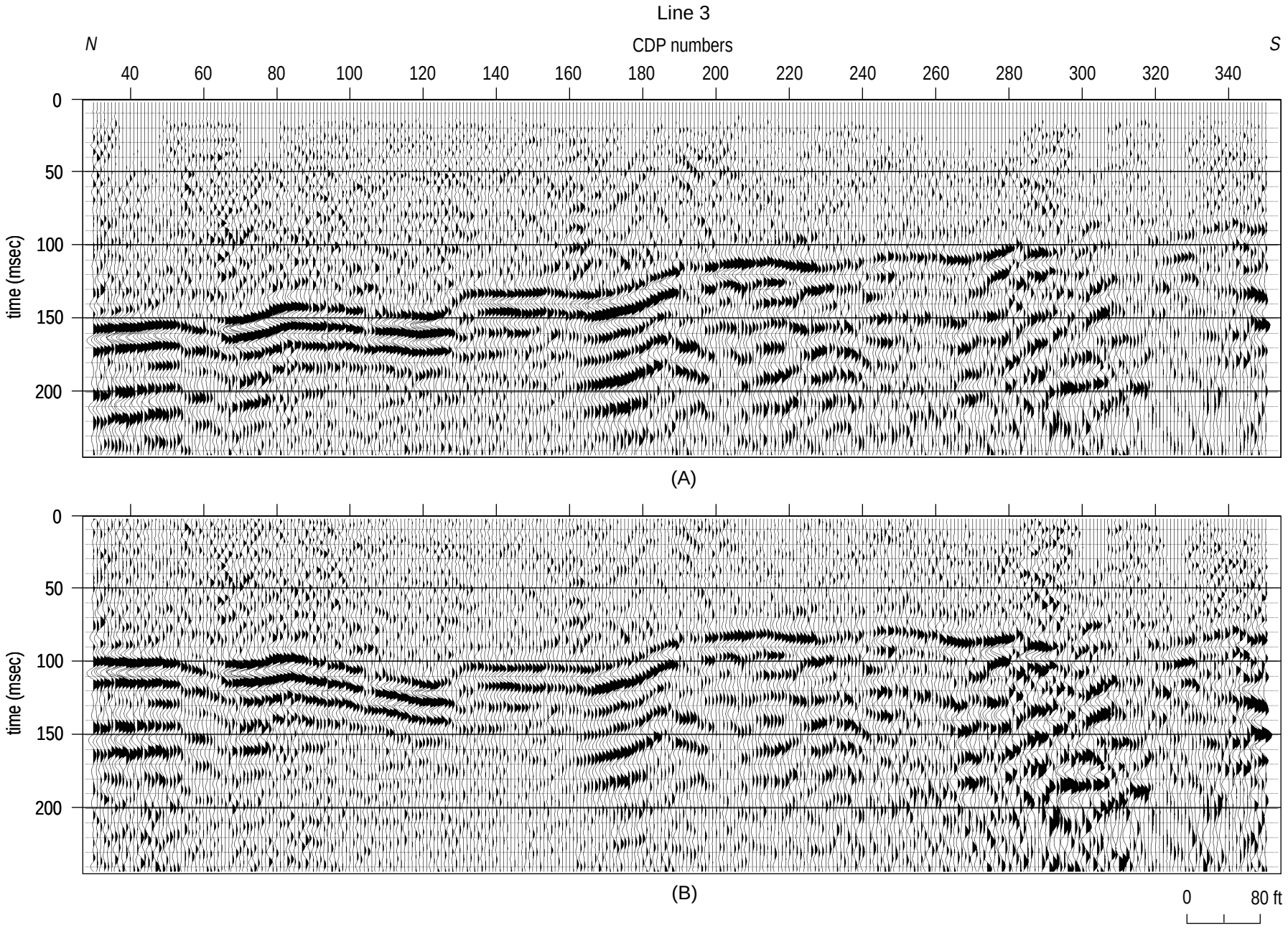
Line 3
N
CDP numbers
S
40
60
80
100
120
140
160
180
200
220
240
260
280
300
320
340
0
50
100
150
200
time (msec)
(A)
(B)
0
80 ft

Figure 8A-B.

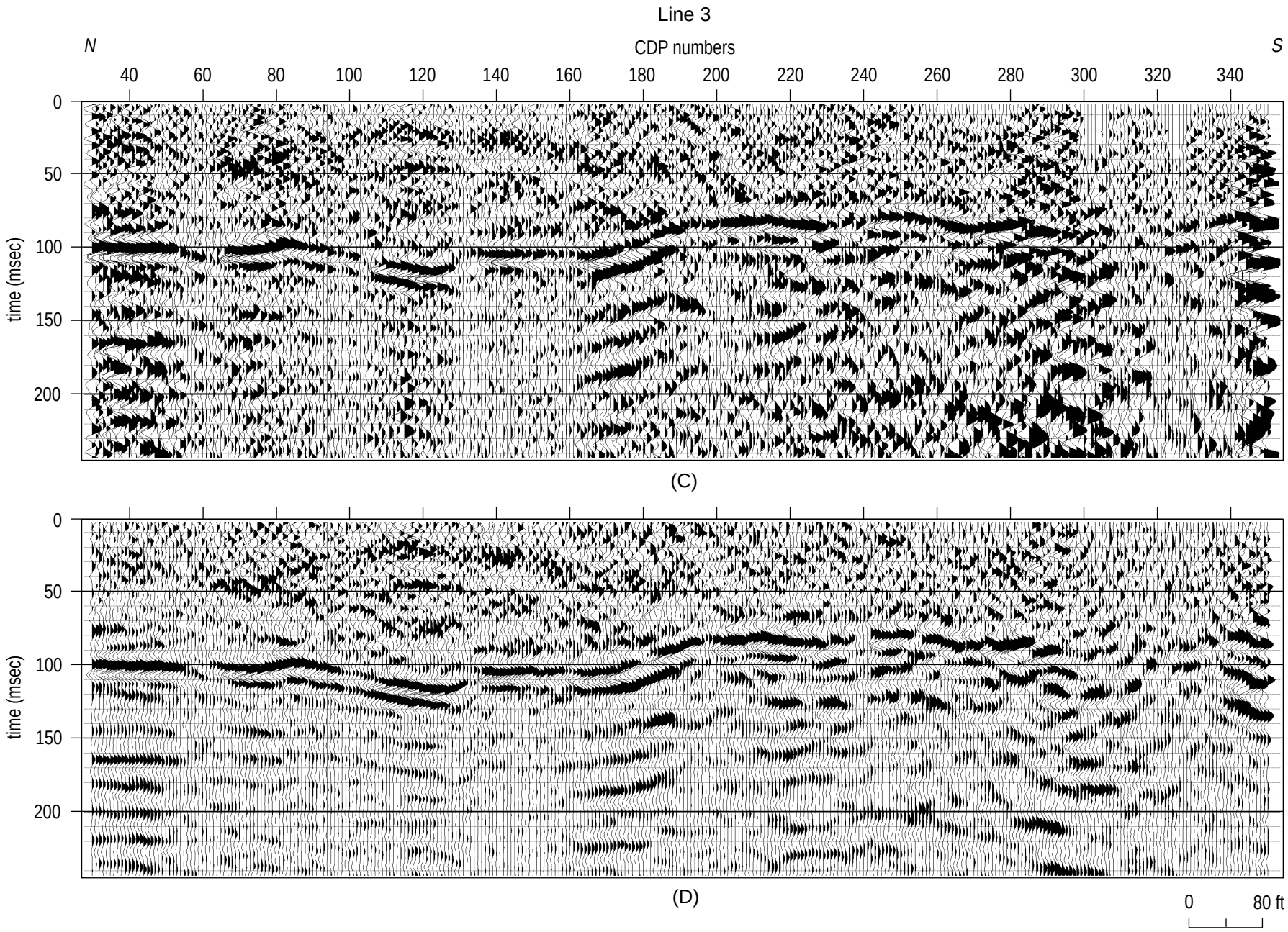
Line 3
N
CDP numbers
S
40
60
80
100
120
140
160
180
200
220
240
260
280
300
320
340
0
50
100
150
200
time (msec)
(C)
(D)
0
80 ft

Figure 8C-D.

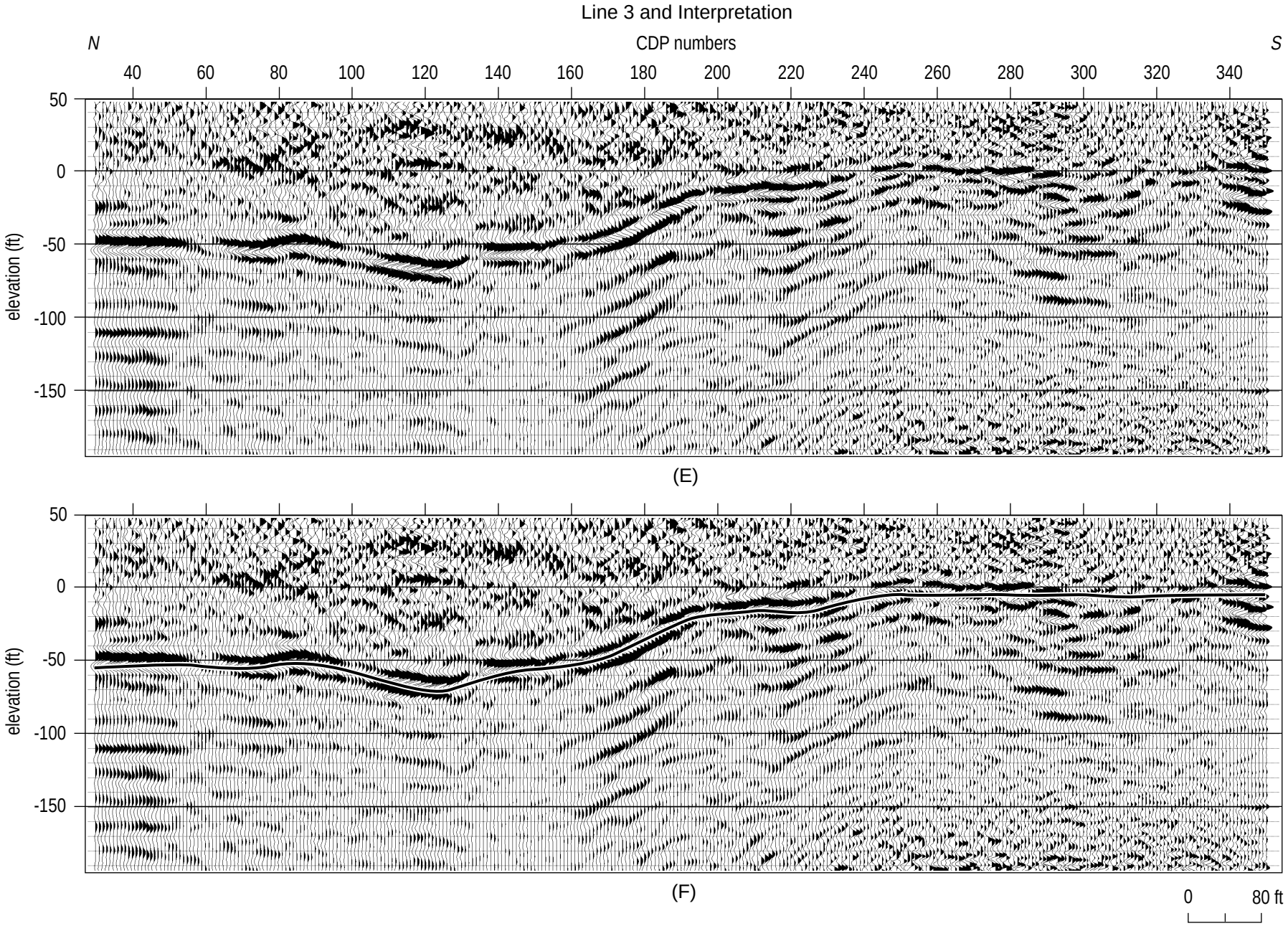
Line 3 and Interpretation
N
CDP numbers
S
40
60
80
100
120
140
160
180
200
220
240
260
280
300
320
340
50
0
-50
-100
-150
elevation (ft)
(E)
50
0
-50
-100
-150
elevation (ft)
(F)
0
80 ft

Figure 8E-F.

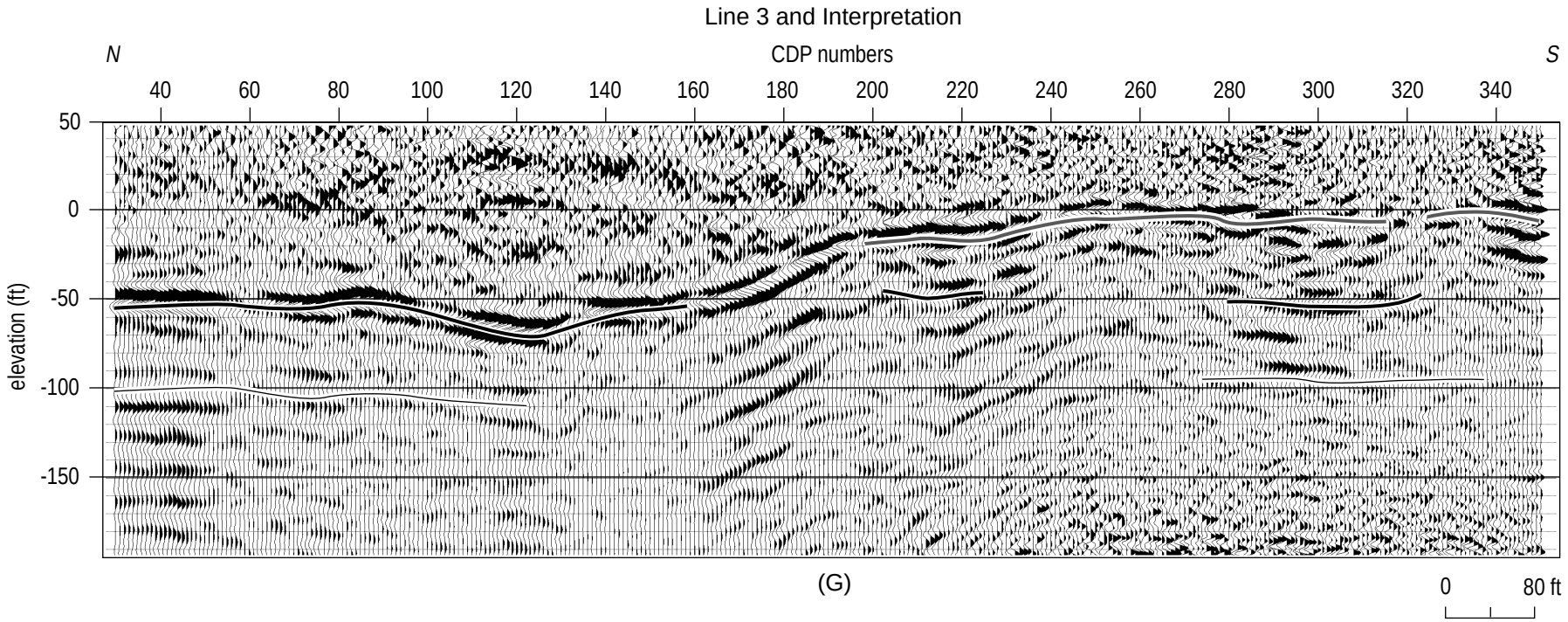

Figure 8A-G. Line 3, 24-fold, CDP stacked section. A) Elevation corrected to multiple sloping datums. B)Same CDP data as (A) elevation corrected to a single flat 48 ft sea level datum. C)Deconvolved (B). D)F-k migrated (C). E)Depth converted (D) using the stacking velocities. F)Interpreted (E) assuming the shallowest reflection is from the same reflector across the line. G)Interpretation of (E) if the shallowest reflection is discontinuous at the apparent offset.

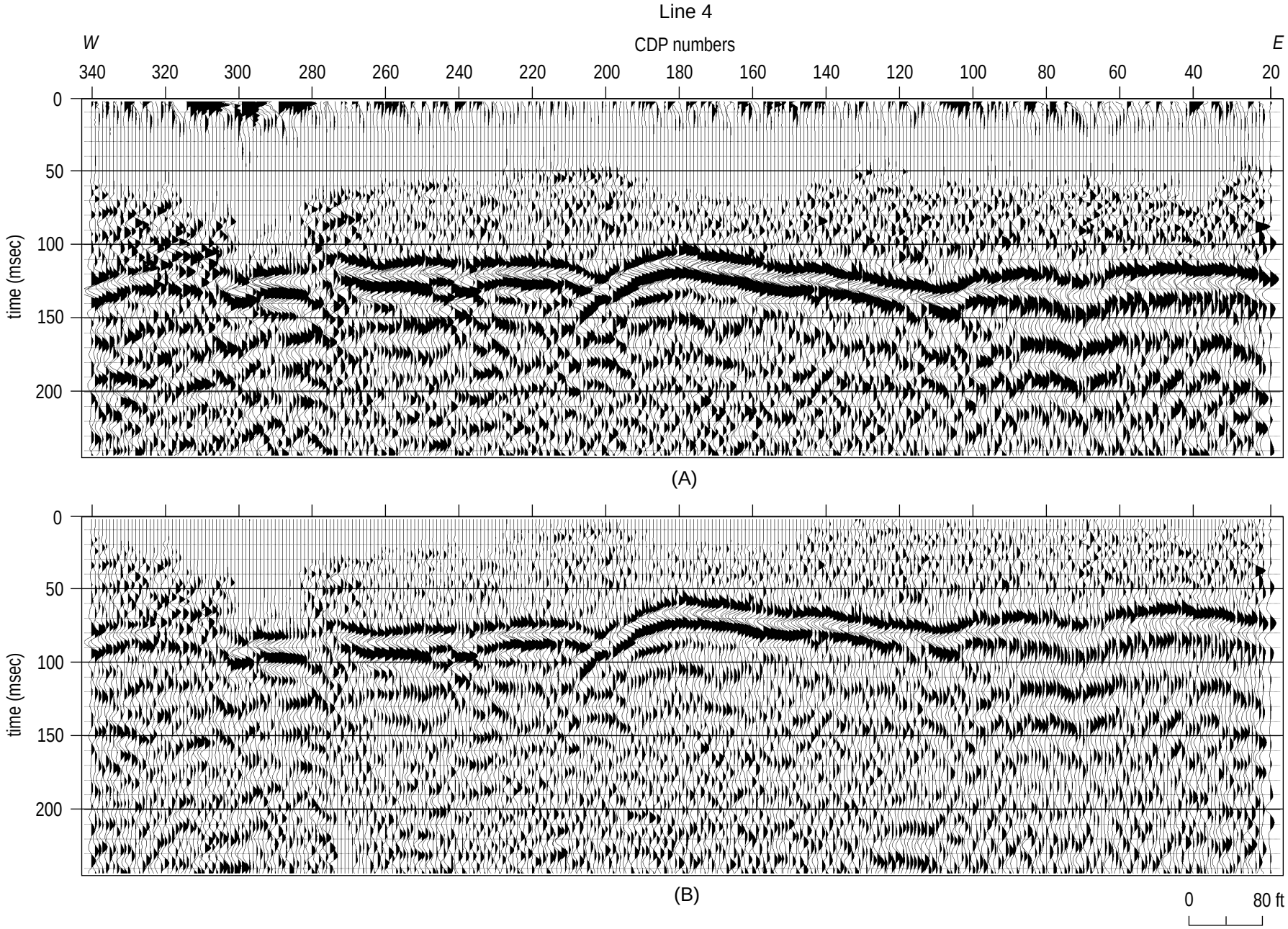
Line 4
W
CDP numbers
E
340
320
300
280
260
240
220
200
180
160
140
120
100
80
60
40
20
0
50
100
150
200
time (msec)
(A)
(B)
0
80 ft

Figure 9A-B.

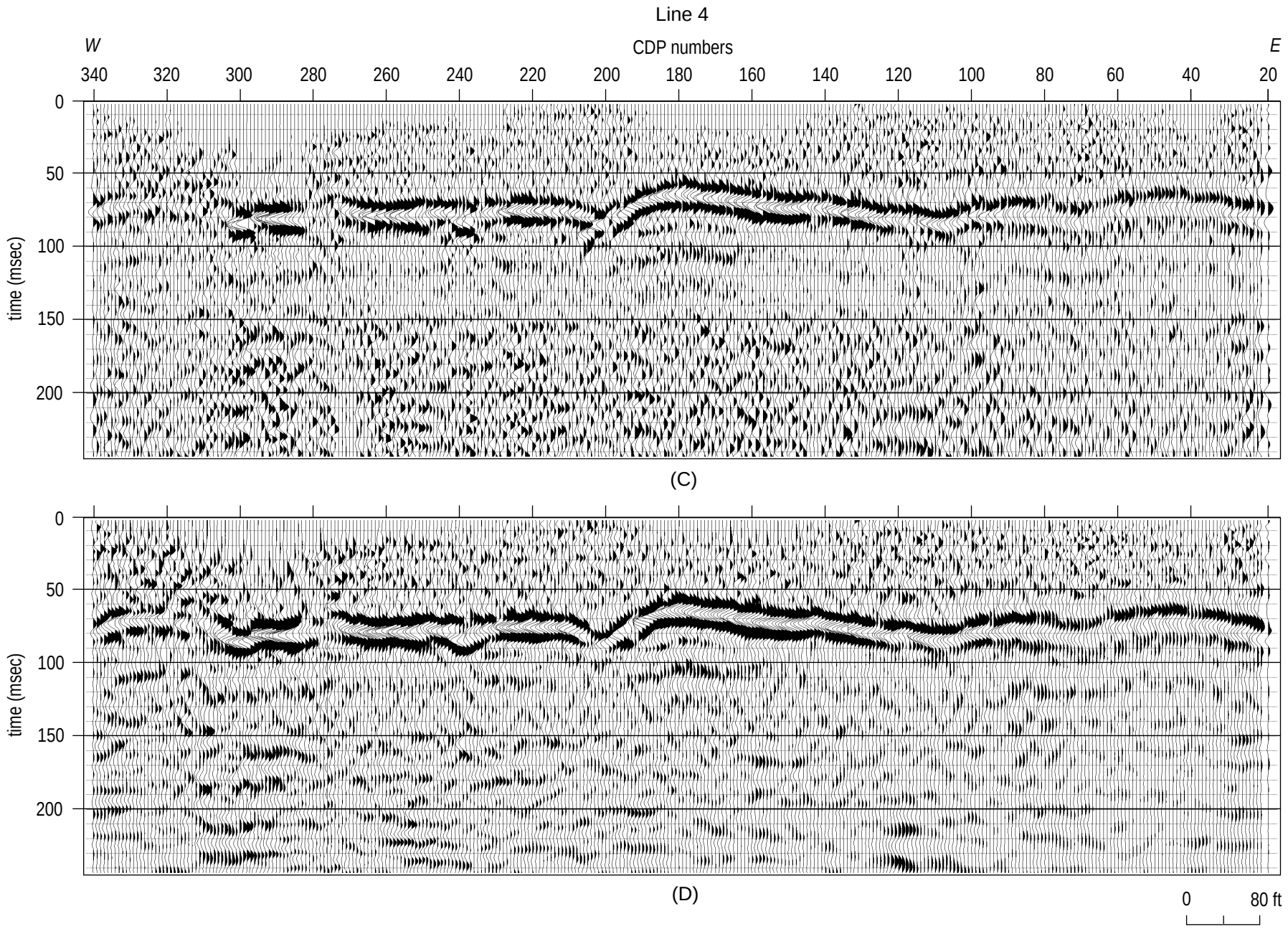
Line 4
W
CDP numbers
E
340
320
300
280
260
240
220
200
180
160
140
120
100
80
60
40
20
0
50
100
150
200
time (msec)
(C)
0
50
100
150
200
time (msec)
(D)
0
80 ft

Figure 9C-D.

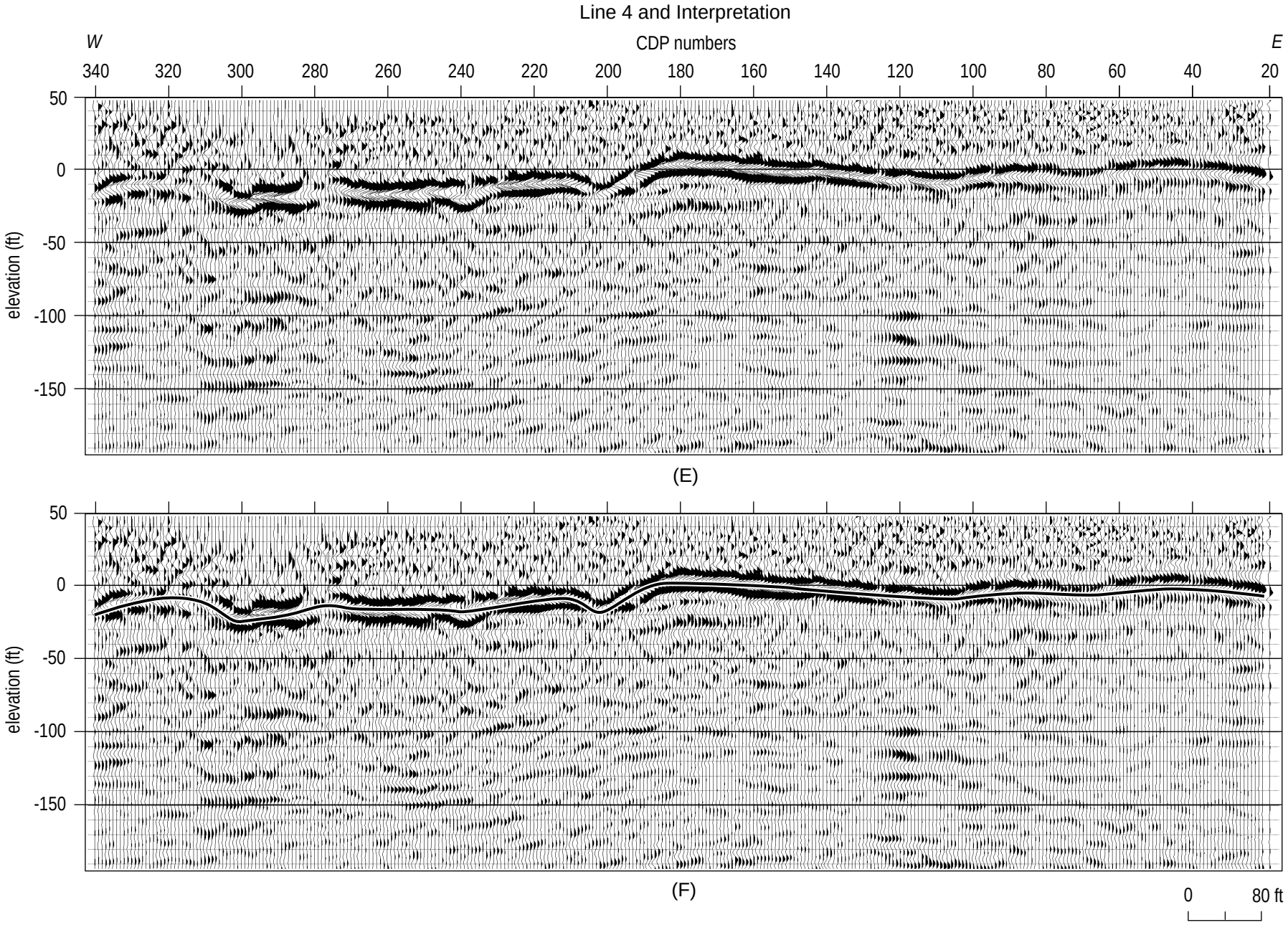
Line 4 and Interpretation
W
CDP numbers
E
340
320
300
280
260
240
220
200
180
160
140
120
100
80
60
40
20
50
0
-50
-100
-150
elevation (ft)
(E)
(F)
0
80 ft

Figure 9E-F.

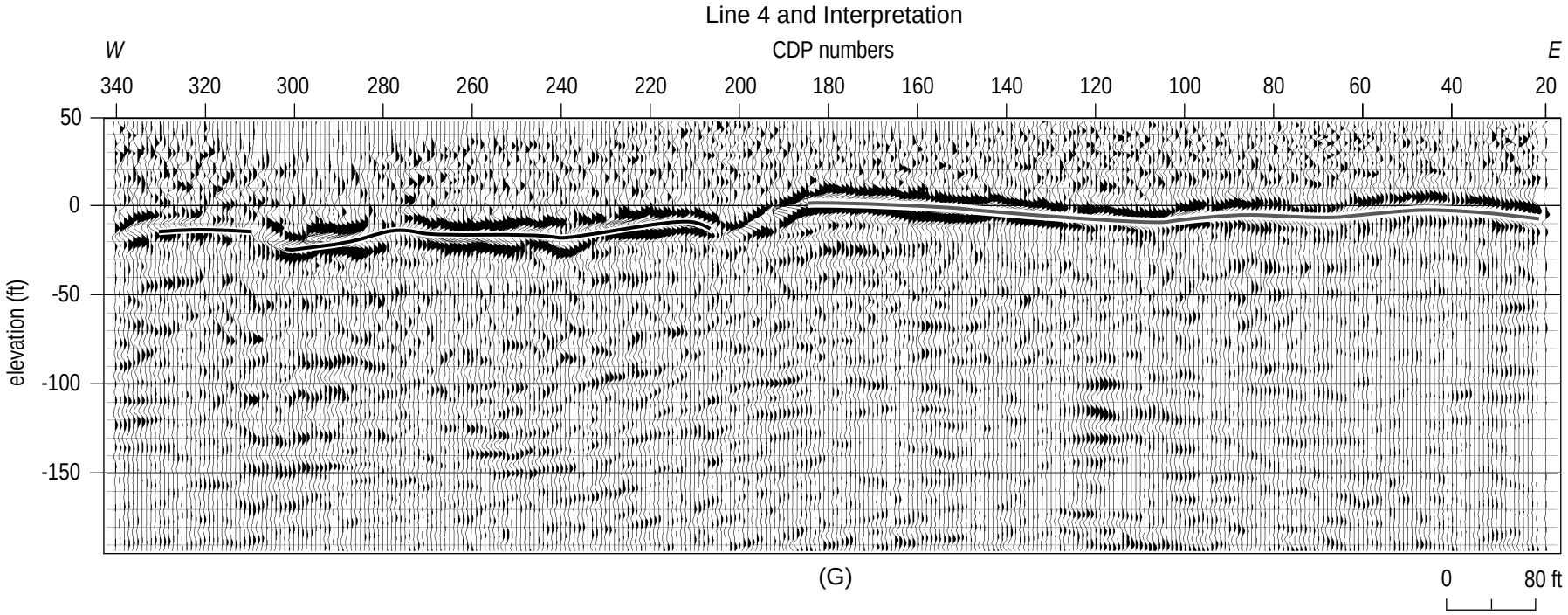

Figure 9A-G. Line 4, 24-fold, CDP stacked section. A) Elevation corrected to multiple sloping datums. B)Same CDP data as (A) elevation corrected to a single flat 48 ft sea level datum. C)Deconvolved (B). D)F-k migrated (C). E)Depth converted (D) using the stacking velocities. F)Interpreted (E) assuming the shallowest reflection is from the same reflector across the line. G)Interpretation of (E) if the shallowest reflection is discontinuous at the apparent offset.

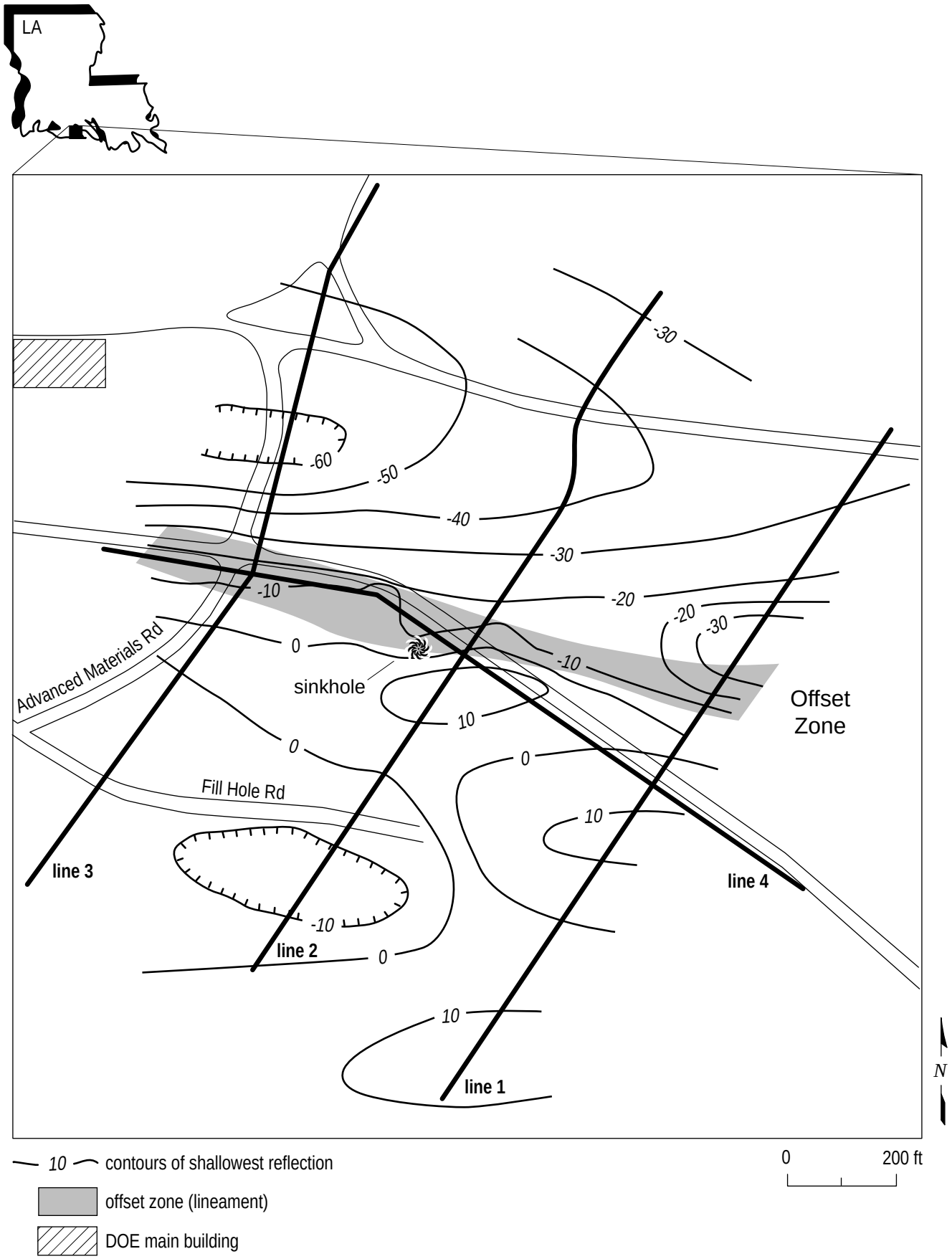

Figure 10. Linear projection of apparent offset and wavelet change on seismic lines 1, 2, 3, and 4. The lineament intersects the sinkhole and the steep sided ditch on line 1. Based on projections from mine maps, the lineament is consistent with the mine face of both the upper and lower cavities. Control points for the shallowest reflection contours are directly extracted from seismic sections 6F through 9F.

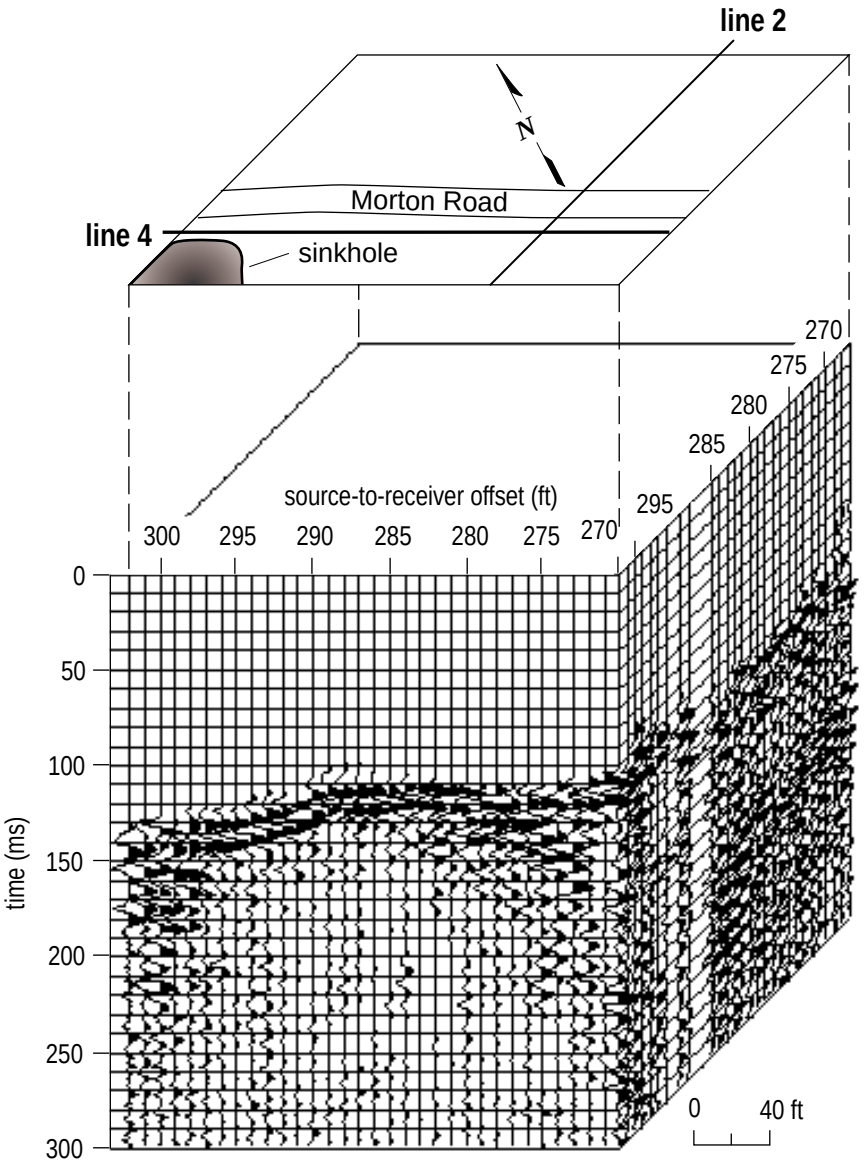

Figure 11. One-fold, 3-D volumetric seismic section with the relative location of the sinkhole and Morton Road overlain. This 3-D slice clearly traces the subsurface expression of the sinkhole. Processing parameters including velocity correction, statics, muting, and filtering were assigned based on analysis of the 2-D data in the immediate area.